AFIT/GEE/ENP/95D-09

STUDY OF THE LONG-TERM DESORPTION OF TRICHLOROETHYLENE FROM CLAY SOILS USING INFRARED SPECTROSCOPY

THESIS

Presented to the Faculty of the School of Engineering

of the Air Force Institute of Technology

Air University

In Partial Fulfillment of the

Requirements for the Degree of

Master of Science in Engineering and Environmental Management

Mary P. Stager, B.S.

First Lieutenant, USAF

December 1995

Acknowledgments

I thank my advisor, Major Glenn Perram for his guidance and leadership throughout this thesis. He was instrumental in designing this research effort and patiently provided assistance and insight whenever needed. His advisement is greatly appreciated. I also thank my committee members, Dr. Bleckmann and Lt. Col. Wolf, for their time, energy and excellent ideas. I thank Jim Reynolds, our Laboratory Technician, for his assistance in getting the apparatus running. I appreciate his time, effort, and patience in helping an environmental student learn the ropes of the physics laboratory.

I thank my family and friends for constant support. My parents, Paul and Marianne Stager, were as always, wonderful advocates full of thoughtful advice. I am truly blessed to have such loving and supporting parents. I also thank my sister Kathleen Hatfalvi for her inspirational encouragement and Charles Sherwin for being such a great motivator. The help from each of them was crucial to this research effort.

Above all, I thank the Lord for the gift of life and the opportunity to learn. I look forward to opportunities in the future where I can use the knowledge and insight gained at AFIT to accomplish the work He has given me to do.

Table of Contents

Page

List of Figures

Figure
Page

List of Tables

Table
Page

Terminology

Absorption - diffusion of a contaminant *into* a soil particle with sorption onto *interior* binding sites.

Adsorption - binding of a contaminant to the *outer surface* sites of a soil particle.

Aquifer - Rock or sediment in the subsurface which is saturated (surrounded by water) and sufficiently permeable to transmit large quantities of water to wells and springs.

Biodegradation - breakdown of a contaminant through metabolism or transformation by microorganisms.

Desorption - release of sorbed contaminants from soil. Refers to the opposite of both adsorption and absorption.

Diffusion - movement of a contaminant from a more concentrated area to a less concentrated area. Pertains to movement into and out of the soil matrix.

Fate - condition of a contaminant affected by physical, chemical, or biological transformations in the environment. (E.g. oxidation, biodegradation)

Gamma distribution - continuous probability density function in which the variable of interest has a skewed distribution.

Soil matrix - complex structure of a soil particle, including both surface and internal sites.

Sorption - movement of contaminants from the mobile phase surrounding soil particles to the immobile phase on soil. Includes both adsorption and absorption.

Subsurface - lying below the ground surface, including soil, groundwater, and the vadose zone.

TCE - Trichloroethylene. A solvent used in degreasing and the primary VOC contaminant at U.S. Superfund sites.

Transport - movement of contaminants in the environment.

VOC - Volatile Organic Compound. An organic compound characterized as highly mobile in the groundwater and readily volatilized into the atmosphere.

Vadose zone - region between the land surface and the water table.

Abstract

The slow desorption of contaminants from soil presents one of the greatest challenges to modeling contaminant fate and transport and implementing effective remediation technologies. The kinetics of long-term desorption of trichloroethylene (TCE) from powdered clay soils were studied to determine the desorption rates and mechanism. Infrared absorption spectroscopy was used to monitor the concentration of TCE desorbed from contaminated flint clay for 71 hours. The observed gas phase TCE concentrations as a function of time were compared to that predicted by a one-site Langmuir desorption mechanism. The Langmuir model, with a single type of bonding site, did not adequately represent the desorption data. It did not account for the release of entrained contaminant past the rapid desorption phase, indicating both the existence of a second phase of slow desorption, and the need for a desorption model based on more than one type of binding site. A second model, based on a Gamma distribution of desorption rate coefficients, fit both the rapid and slow desorption phases, representing the entire desorption profile. The application of infrared absorption spectroscopy to measure long-term desorption in the environmental field is demonstrated. This method allowed continuous measurement of desorption over long time periods (days). A multiplex design in the optical detection system improved measurement capabilities, allowing quantification of contaminant to 0.06 torr of TCE. The ability to measure such small changes in contaminant concentration is an important development in characterizing and understanding long-term desorption trends.

STUDY OF THE LONG-TERM DESORPTION OF TCE FROM CLAY SOILS USING INFRARED SPECTROSCOPY

Chapter I - Introduction

General Issue

Contamination of the subsurface environment is a problem encountered in every state of the country and at numerous Air Force Bases. Due to their widespread use across industry and commerce, volatile organic compounds (VOCs) are often the primary pollutant in contaminated areas (Siegrist, 1992: 3-4). Trichloroethylene (TCE), a common VOC, was found in 35% of the Superfund sites across the United States, showing to be the most prevalent contaminant (Siegrist, 1992:4). Containment and clean-up of VOC-contaminated sites rely on understanding contaminant fate and transport and implementing effective clean-up technologies. The greatest challenge to current remediation technologies is slow transport of VOCs from the soil resulting in a substantial quantity of contaminant retained in the soil matrix (Crotwell et al., 1992: 36).

Desorption is the release of adsorbed contaminants from soil. Studies indicate that desorption is the rate-limiting step in remediation efforts (Ball, 1991:1237; Pavlostathis and Mathavan, 1992:537; Crotwell et al., 1992:37). Desorption is believed to proceed via a two-phase process: the first is rapid, short-term removal of the contaminant from the surface of the soil particles within 24 hours; and the second phase is a slow, long-term process controlled by slow diffusion of molecules from the interior of the soil matrix

(Grathwohl and Reinhard, 1993:2365; Pavlostathis and Mathavan, 1992:534). It is this slower mechanism which is believed to limit contaminant release, causing a significant fraction of contaminant to remain in soils and groundwater, frustrating remediation efforts. Understanding the kinetics of slow desorption is important for predicting contaminant fate and transport and improving clean-up technologies.

Motivation

Increasing the understanding of the desorption mechanism has a number of benefits. These benefits lend themselves to fate and transport characterization, the development of more realistic models and clean-up time estimations, and the implementation of proper clean-up techniques. Understanding the desorption mechanisms that cause the slow release of contaminants from soils is important to minimizing costs and schedule risks to the Air Force.

Reliance of Models on Desorption

Project management risks, (cost, schedule and performance) rely on the adequate representation of contaminant behavior through modeling. Models are used throughout the United States and in the Air Force to forecast the fate of environmental contaminants, predict contaminant flow and transport, choose appropriate clean-up technologies, and estimate site clean-up times.

Desorption can be the rate-limiting step in fate processes. Fate processes include any chemical, biological or physical transformation. Many fate mechanisms rely on the

availability of compounds in the non-sorbed state. For instance, fuels trapped in the micropores of soil are largely inaccessible to added nutrients and oxygen (Downey and Elliott, 1990: 171). Biodegradation of such contaminants is limited by slow diffusion from interior soil sites that are inaccessible to microbes (Pignatello, 1989: 71).

Desorption of pollutants is also linked to contaminant transport. Cho observed that desorption from soil was the dominant process affecting TCE transport in the field (Cho, 1993: 3340). Data from the study of the desorption mechanism is necessary to accurately predict the transport of contaminants, which in turn, are key to developing realistic models and accurate clean-up time estimations. Study and characterization of desorption aids in the development of models for predicting the fate and transport of organics in the environment.

Reliance of Remediation Technologies on Desorption

Study of the slow desorption rate can lead to better efficiency in the clean-up of TCE-contaminated aquifers. Desorption characterization aids in the selection and improvement of appropriate clean-up technologies. Clean-up strategies for TCE and other contaminants have been limited by the slow extraction of VOCs from groundwater and soil. The principal limitation is slow desorption of the compound from the soil matrix (Grathwohl and Reinhard, 1993: 2360).

The pump and treat technology draws out groundwater from an aquifer and treats it to remove contaminants. This strategy relies on the presence of molecules in the mobile state. Retardation of contaminants through slow desorption increases both the time

required to achieve clean-up standards and the volume of water needed to flush the contaminated area (Mackay and Cherry, 1989: 633). The result is both additional cost and schedule risk to the Air Force in achieving a clean environment. These costly effects can be minimized by greater understanding of the desorptive kinetics between the soil type and contaminant.

Vapor Extraction is an in-situ soil process that removes VOCs from the vadose zone of soil. A VES (Vapor Extraction System) provides a moving air stream that volatilizes contaminants and draws them to the surface. A vacuum produces an air flow that sweeps out the soil gas. VES is effective in removing contaminant in the free liquid, vapor, and surface sorbed phases. Contaminant diffused into the interior of the soil matrix, however, are the most difficult to extract, and pose the greatest challenge to current remediation technologies (Crotwell et al., 1992: 36).

Past Research Efforts

Research has indicated that desorption of contaminants is affected by the following soil properties:

- Soil type and surface area (Kindt, 1994:65; Kreamer et al., 1994:355; Ong and Lion, 1991a:183).
- Water content of soil (Ong and Lion, 1991a:183; Ong and Lion, 1991b:1565-1567; Smith et al., 1990:680; Thibaud et al., 1993:2373).
- Ionic strength (Estes et al., 1988: 380).

- Temperature (Fares, 1994:85; Farrell and Reinhard, 1994:68).
- Soil pH (Estes et al., 1988: 380).
- Resident time of contamination (Connaughton, 1993:2400; Li and Gupta, 1994:133).

Recent research has focused on determining short-term rates for desorption of TCE and characterization of the rapid mechanism. Fares, Kindt, and LaPuma demonstrated that the short-term desorption rate varies with temperature, (Fares, 1994:85), soil type, and particle surface area (Kindt, 1994:65, 76-77). Contaminant residence time (up to 19 hours) did not appear to affect the short-term desorption mechanism (LaPuma, 1994:75-76, 84-85).

Fares, Kindt, LaPuma and Perram demonstrated that the Langmuir kinetic mechanism is a valid model for representing the initial, rapid desorption mechanism. Their findings focused on the first five hours of desorption (Fares et al., 1995:1566-1568). Figure 1 illustrates the desorptive release of TCE over a short term. The pattern shown in this figure is similar to the shape of the Langmuir Kinetic model. (This model is described in detail in Chapter 2. It is introduced here briefly to demonstrate past research findings.)

In the Figure 1, the x-axis is time and the y-axis is the concentration of desorbed TCE. The rate of desorption is rapid at first, followed by a gradual decrease until steady-state is reached and desorption reaches an asymptotic value. At this point, $d[TCE]/dt = 0$ and no additional contaminant is released from the soil.

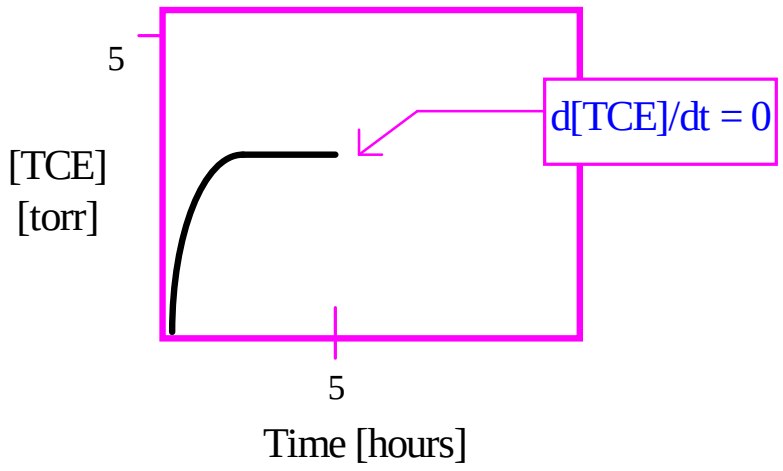

Figure 1. Short-Term Desorption Pattern
(Shape of One-Site Langmuir Model)

This figure and the Langmuir Kinetic Model focus on the short-term, rapid desorption mechanism, which occurs within 1-24 hours. Further research examining the desorption mechanism over longer periods of time is needed to model the extended release of contaminants from soil.

Problem Statement

This research effort investigates the extended release of contaminants by continuously monitoring desorption over run times greater than the rapid desorption phase. Infrared spectroscopy is used to monitor desorption and improvements to the optical apparatus are developed to increase the limit of detection. The desorption data is

fit to a kinetic model to determine whether the long-term desorption mechanism is governed by a single type of binding site, or more than one type of release mechanism.

Research Objectives

To facilitate greater understanding of desorption kinetics, this research effort has three objectives.

1) Investigate the long-term desorption mechanism of TCE from flint clay. The long-term mechanism is analyzed by determining if the desorption mechanism relies on a single desorption rate or multiple rates.

The Langmuir mechanism assumes a single type of bonding site with a single desorption rate. It predicts a steady-state adsorption/desorption condition after a short period of time. Perhaps the desorption mechanism, rather than being dependent one binding site, is dependent on two, three, or more types of binding sites yielding more than one desorption rate. If there is more than one desorption rate, then desorption monitored over long periods of time (days), would not reach steady-state but show continual contaminant release.

The supposition of more than one binding site and desorption rate can be tested by applying a one-site Langmuir model to long-term desorption data. If the model fits the desorption data, then the theory of a single binding site and desorption rate is reinforced. If the Langmuir model does not fit well, this may indicate that there is more than one type of binding site and more than one desorption rate. This may also indicate that another

mechanism exists (slow kinetics, mass transfer or diffusion) which affects contaminant release and may greatly affect contaminant removal. Lack of fit by the one-site Langmuir model would also indicate the need for another model that could adequately describe the desorption trend over longer time periods.

The desorption of TCE will be monitored for greater than 70 hours; longer than the rapid desorption phase, to see if the concentration of TCE reaches an asymptotic value or continues to increase with time. If it reaches steady-state, a pattern similar to Figure 1 will be observed. If it continues to increase, a pattern similar to Figure 2 (below) could be observed. This pattern indicates there is more than one release mechanism acting on the contaminant. Figure 2 shows that instead of reaching a steady-state value, d[TCE]/dt > 0, and the concentration of TCE continues to increase with time.

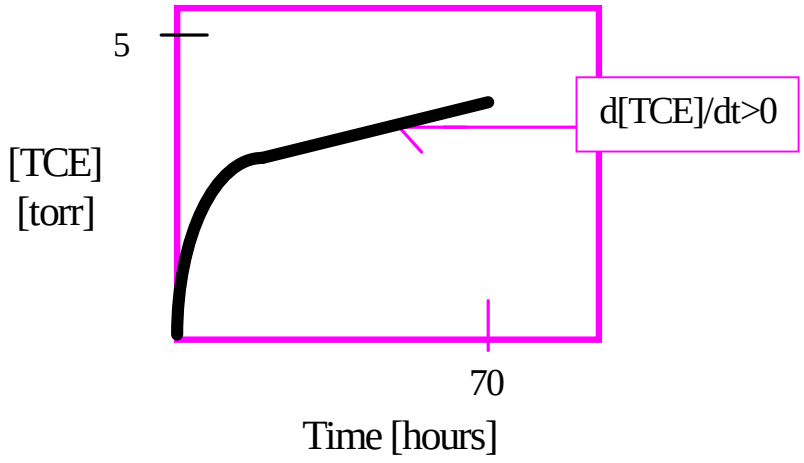

Figure 2. Possible Long-Term Desorption Pattern

If a long-term desorption pattern similar to Figure 2 is observed and the Langmuir model fit is not adequate, then a second model will be investigated to represent the long-term desorption pattern.

2) A second objective of the research is to use continuous data acquisition to investigate the long-term desorption rate. Continuous measurement of desorption over time is a unique capability offered by the optical technique employed in this research, infrared spectroscopy. Traditional desorption rate measurement techniques include: the EPA-recommended purge and trap extraction (Siegrist, 1992:11; Connaughton et al., 1993:2398); centrifugation followed by solvent extraction (Smith, 1990:679; Li and Gupta, 1994:129; Pavlostathis and Jalgal, 1991:275-277); and thermal desorption (Sawhney et al., 1988:150). The amount of desorption for most techniques is quantified by gas chromatography. The limitation of these traditional testing techniques is two-fold. First, purge and trap techniques often fail to quantify the amount of contaminant entrained in the soil matrix (Sawhney et al., 1988:150; Travis and Macinnis, 1992:1886; Reeder, 1993: 90). Second, each of the measurement techniques mentioned above focus on a snapshot in time. A sample of contaminated soil or water is pulled from the remaining population and subjected to the testing techniques. The amount of desorbed contaminant is measured for that *single* time at which the sample was pulled. Most measurements are separated by at least 1-20 hours between samples. Continuous quantification of desorption is limited by the time required to prepare and send each sample through a chromatograph. Optical absorption techniques may offer an alternative method to

measure desorption rates, allowing continuous measurement over extended periods of time.

3) The third objective in this research effort is to improve the optical design for desorption rate measurements and enhance the limit of detection for long-term desorption observations. The limit of detection is the minimum concentration that can be detected by the apparatus. Traditional measurements (those mentioned in Objective 2 above) are often unable to quantify long-term desorption rates because of a poor detection limit. Some desorption experiments are unable to quantify minute increases in desorbed contaminant. (Pavlostathis and Jaglal, 1991:276) It is difficult to measure minute changes in contaminant concentration without introducing measurement error. This research effort seeks to establish a method of contaminant measurement which can detect minute changes in long-term desorption data. The third objective is aimed at improving the limit of detection through optical design.

Overview

The remainder of this thesis begins with an overview of the contaminant in study and its behavior in the subsurface. Chapter 2 continues with the theory necessary to analyze the data. Chapter 3 focuses on the experiment design and improvements made to the apparatus. Chapter 4 presents the results from a long-term data and measurement improvements gained from apparatus design. This chapter discusses the adequacy of two different models for describing long-term desorption. The last chapter will review the research objectives, providing conclusions on: the long-term desorption mechanism, the

application of models to describe the desorption profile, the adequacy of optical techniques to measure desorption, and the significance of improvements in experimental design. Finally, recommendations will be made for general improvements and further research. A glossary of technical terms and acronyms used in this thesis is located in the prefatory pages. Full derivation of models and supportive information to the research is included in Appendices A-H.

Chapter 2 - Background

Introduction

Trichloroethylene (TCE) was a major industrial solvent from 1940 to the late 1970's, used extensively across the Air Force until its carcinogenic effects were discovered. This volatile organic compound (VOC) was used as a degreaser in aircraft parts and electronic components (Schaumburg, 1990:17; Avon and Bredehoeft, 1989:25-26). Entry into the environment occurs though a number of pathways. Inappropriate disposal methods such as disposal into shop drains and open drainage ditches; leaking underground tanks, sewage pipes and landfills; and releases from metal-degreasing facilities have all led to extensive contamination to the environment from TCE. These releases of TCE over the past 50 years have led to groundwater and soil contamination at numerous Superfund sites and several Air Force Bases (Avon and Bredehoeft, 1989:25; Stimpson, 1989:36; Hylton, 1992:54).

Behavior of TCE in the Subsurface

Once in the groundwater, TCE can cause extensive contamination of an aquifer, even destroy a drinking water source. A relatively small volume of TCE can have a severe impact on groundwater quality (Avon and Bredehoeft, 1989:47). At an airport in Denver, CO, 80 liters of contaminant spread to create a 4 1/2 billion liter plume of contaminated groundwater (Mackay and Cherry, 1989:631). At Castle AFB, CA, 100 gallons of TCE caused extensive contamination, with concentrations of 175 μg/L in the groundwater.

Note, the Maximum Contaminant Level (MCL) for trichloroethylene in drinking water is 5 μg/L (Bourg, 1992:365). The plume at Castle AFB poses a significant threat to nearby drinking water wells, which are in the path of groundwater flow (Avon and Bredehoeft, 1989:35).

Sources of TCE Contamination

To characterize contaminant flow and release mechanisms, one must understand where the prominent sources of the contaminant are in the subsurface. A crucial step in any clean-up process is identifying and eliminating the sources of contamination. This is first accomplished by removing the original sources (such as those mentioned above) that serve as discharges of TCE. However, even after the original source has been attended to, the possibility for further contamination still exists. Once an organic is released to the subsurface, it may congregate as residual in the unsaturated zone or as pools on top or beneath aquifers, forming a secondary source. The soil matrix can also act as a secondary source, behaving as an irreversible "sponge". Contaminants absorb onto and into the soil but desorb out of the soil at a much slower rate. The soil may retain a significant fraction of contaminant and slowly release it over extremely long periods of time. These secondary sources can continually add contaminant to the soil vapor and groundwater over a long time (Mackay and Cherry, 1989:631). Characterization of their release of contaminant is crucial to predicting fate and transport processes (Pignatello, 1989: 70-74).

Transport of TCE in the Subsurface

Knowing a contaminant's flow characteristics and its likely travel pathways is necessary to characterize its behavior in the subsurface. As a dense chlorinated organic, TCE has specific properties that govern its movement in groundwater. TCE is an unsaturated, chlorinated aliphatic compound with a low molecular weight (131.4 g/mole). It has a high density (1.46 g/ml), low surface tension, and high vapor pressure (Government of Canada, 1993:4). It is only slightly soluble in water, and as a DNAPL (dense non-aqueous phase liquid), it tends to sink in groundwater. When released into the ground, TCE can migrate rapidly through the unsaturated zone, especially if the soil is dry. It leaves behind droplets of organic liquid in the pore spaces and some adsorbs to the soil particles while the rest is pulled downward by gravity (Bourg et al., 1992:359). When it reaches a less permeable layer or the groundwater table, its downward movement is slowed and it collects on top of the layer, building up in TCE-hydraulic head. This will force the TCE to spread laterally. If the hydraulic head of the TCE is great enough to overcome the retention capacity of the unsaturated zone and the entry-pressure needed to penetrate the aquifer surface, the excess mass of TCE will force itself into the saturated zone (Bourg et al., 1992:3; Schwille, 1988:7-8). Once in the groundwater, TCE continues downward. Impermeable strata encountered in its pathway can again cause lateral spreading of the contaminant. If the retention capacity of the saturated zone is also exceeded, the TCE will spread and collect in basins and depressions along the bottom of the aquifer. Here it can form pools and puddles, which serve as secondary sources of contamination. Groundwater that flows over the pools and puddles will transport the

TCE horizontally across the aquifer (Schwille, 1988:8). Between deposition on soil and collecting in pools and spreading, it is evident that there are many pathways for TCE to follow in the subsurface and into the groundwater.

Partitioning of TCE in the Subsurface

When VOCs enter the subsurface environment, they can reside in five different phases within the soil matrix (Crotwell et al., 1992:36; Travis and MacInnis, 1992:1886):

1. Vapor phase in voids of air surrounding soil
2. Free liquid phase between soil particles (Free product)
3. Dissolved in water surrounding the soil
4. Adsorbed to the surface of soil particles
5. Sequestered/entrapped in the interior of the soil matrix

The first three phases (vapor, free liquid, and dissolved) are relatively easy to remove from contaminated aquifers and vadose zones. Molecules in these non-sorbed states are mobile and easily transported by air or water flow out of the subsurface. Vapor and groundwater extraction systems rely solely on the presence of molecules in the non-sorbed state. The molecules are also accessible to microorganisms for biodegredation. However, contaminants sorbed to the soil matrix appear to withstand common treatment techniques. Microorganisms are less able to assimilate and transform sorbed molecules than mobile molecules (Pignatello, 1989:45). The release of contaminants adsorbed within the soil matrix is controlled by the slow desorption mechanism. Understanding of the

equilibration rates and contaminant distribution between these phases is key to developing appropriate remediation techniques.

A study by Travis and MacInnis indicated that at equilibrium, a significant fraction of the total contaminant resides in the interior of the soil matrix (Travis and MacInnis, 1992:1886). Figure 3 illustrates the distribution of 30 L of TCE in one cubic meter of soil. The five phases of contaminant are shown along the x-axis. The soil matrix entraps 37% of the total contaminant. Once the free product is removed, (usually the first step in remediation) it was determined that 22% of the original contaminant mass was still held within the soil matrix.

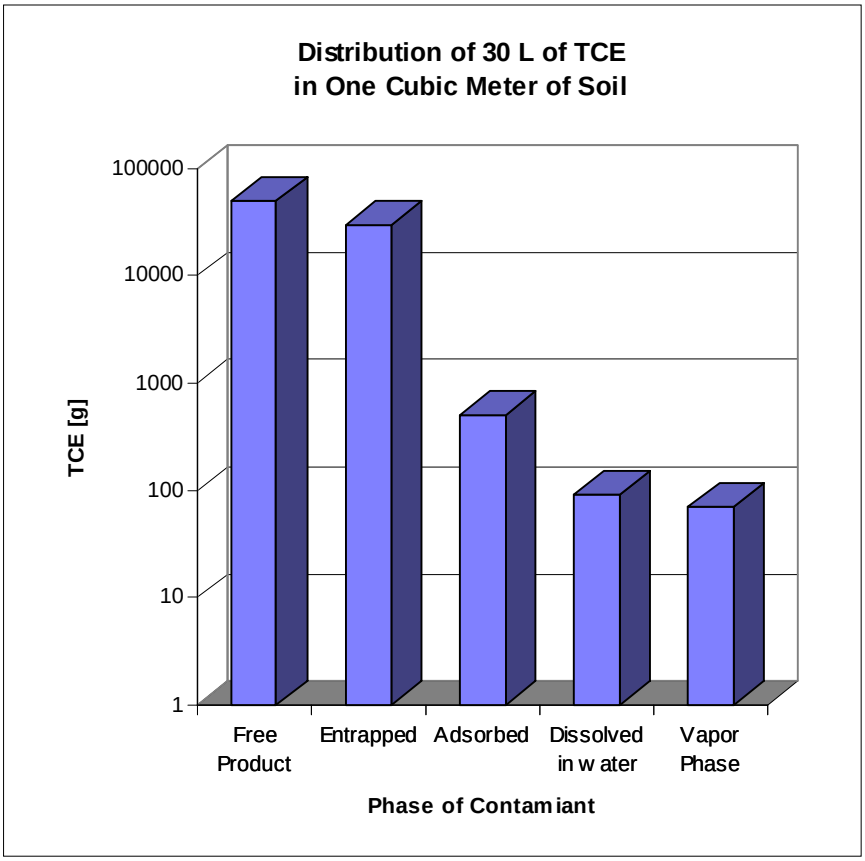

Figure 3. Distribution of TCE in the Subsurface.
(Travis and MacInnis, 1992:1887)

Another study by Sawhney and others showed the resistivity of contaminant removal in long-contaminated soils. The study tested field soils in which the pesticide EDB (1,2-Dibromoethane) had been used as a fumigant. The purge and trap analysis, which relies on the volatilization of the contaminant for measurement, failed to detect 99% of the total contaminant (Sawhney et al., 1988:150; Reeder, 1993:14). Even after vigorous extraction conditions of higher temperatures and longer purging times, 89% of the contaminant remained entrapped in the soil matrix (Sawhney et al., 1988: 150).

The Desorption Process

Researchers have shown that the desorption mechanism of VOCs from soil is a two-phase process (Crotwell et al., 1992:37; Li and Gupta, 1994:132; Farrell and Reinhard, 1994:71). The first phase is rapid desorption, yielding the release of 10 to 70% of contaminants within 24 hours. Rapid desorption begins immediately, with release of contaminant from the outer surfaces of the soil. Researchers have shown rapid desorption to subside in the range of 10 minutes to 24 hours, depending the measurement and extraction technique (Connaughton et al., 1993:2400; Pavlostathis and Mathavan, 1992:534). The second phase is slow desorption. Particles entrained in the soil matrix diffuse slowly, and contaminant may be released days or months after initial desorption. Following rapid desorption, up to 90% of the original sorbed mass may still remain in the soil matrix, contributing to a significant amount of slowly desorbing material (Pavlostathis and Mathavan, 1992:537).

The existence of more than one desorption phase suggests the need for mathematical models which can describe the different phases. As mentioned in Chapter I, the Langmuir one-site model adequately describes the rapid desorption mechanism and can be used as a test to determine if the full desorption mechanism relies on a single type of binding site. Continual release of contaminant (past a rapid phase), however, requires a more complex analysis than the one-site model. A model utilizing two, three or more binding sites for sorption would be needed to describe any contaminant release beyond the rapid phase.

Theory Behind the Experiment

The following sections detail the mathematical relationships used to interpret experimental data. The Langmuir one-site kinetic mechanism describes the relationship between sorbed and non-sorbed contaminant. The Langmuir Kinetic model is introduced to test the long-term desorption mechanism. (Additional derivation for the Langmuir Kinetic model can be found in Appendix A.) Theory related to the optical measurement of desorption is presented next. The Beer-Lambert Law is used for interpreting TCE concentrations from light intensity measurements. The Ideal Gas Law is used to find the cross-sectional area for optical absorption. Determination of the TCE cross-sectional area is discussed at the end of this chapter.

Introduction to the Langmuir Kinetic Mechanism

The desorption mechanism is explored by looking at a model of the Langmuir kinetic mechanism for a single type of binding site. The following illustration shows the relation between the gaseous (free state) and sorbed state of TCE (Perram, 1995):

$$\mathbf{TCE} + \begin{array}{c}| \\ \text{-- S --} \\ |\end{array} \underset{\mathbf{k_d}}{\overset{\mathbf{k_a}}{\rightleftharpoons}} \begin{array}{c}| \\ \text{-- S --} \\ | \\ \mathbf{TCE}\end{array} \qquad (1)$$

where: TCE = Vapor concentration of TCE

S = Soil Particle

| or -- = Site for adsorption (binding site) on soil particle surface

k_a = Rate coefficient for adsorption onto a site

k_d = Rate coefficient for desorption from a site

The left side of the equation shows TCE in a mobile, non-sorbed state and a soil surface with vacant sites. The right side shows a molecule of TCE sorbed to the soil surface. If one assumes there are multiple sites with the same binding energy available for adsorption on a soil particle, then the right side of equation (2) can be represented as θ, the fraction of sites with TCE adsorbed:

$$\theta = \frac{\textbf{\# sites with TCE adsorbed}}{\textbf{total \# of sites in soil}} \qquad (2)$$

If one further assumes that there exists one rate of adsorption for all sites and one rate of desorption for all sites, then a change in θ equates to a change in contaminant concentration. The rate of *increase* in gaseous phase TCE, driven by the fraction of sorbed sites θ, and the rate coefficient for desorption k_d, is shown as follows:

$$\frac{d[TCE]}{dt} = k_d\theta \qquad (3)$$

The rate of *decrease* in gaseous phase TCE, dependent on: the fraction of sites available for adsorption $(1-\theta)$; the concentration of gaseous phase molecules; and the rate coefficient for adsorption, is:

$$\frac{d[TCE]}{dt} = -k_a(1-\theta)[TCE] \qquad (4)$$

A *net* increase in the gaseous phase concentration of TCE can be represented by combining the two equations above:

$$\frac{d[TCE]}{dt} = k_d\theta - k_a(1-\theta)[TCE] \qquad (5)$$

Sorption Equilibrium

The Langmuir Isotherm describes the fraction of soil covered by sorbed contaminant at steady-state, when the rates of adsorption and desorption are at equilibrium:

$$\theta = \frac{K_L C_V}{1 + K_L C_V} \qquad (2)$$

where: θ = fraction of soil sites occupied by the contaminant

K_L = ratio of adsorption and desorption rate coefficients = k_a / k_d

C_V = TCE concentration in the vapor phase = [TCE]

(Morel and Hering, 1993:514-516). This hyperbolic relationship is useful in interpreting adsorption and desorption data. When $\theta = 1$, the soil surface sites are saturated with contaminant. As a soil surface *becomes* saturated with contaminant ($\theta \rightarrow 1$) the rate of adsorption decreases, asymptotically reaching the saturation level. This isotherm is limited to describing sorption only at the surface of the soil particle: slow diffusion into and out of the soil matrix is not accounted for.

The Langmuir Kinetic Model

The TCE concentration can be related to the number of available sorption sites on the soil. A decrease in the number of gaseous phase TCE molecules will result in a direct increase in the number of sorbed soil sites. The rate of desorption from contaminated soil can be found by monitoring the change in TCE concentration in a sample cell over time. The following model describing desorption kinetics was derived to find k_d from the experimental data (Perram, 1995). Appendix A contains the derivation of this model. Key assumptions were made in developing the governing equation for the model. These include:

- All soil sites have the same binding energy to contaminant molecules. (There is a single adsorption rate and a single desorption rate for all sites.)
- The initial gaseous phase TCE concentration in the cell is zero ($[TCE]_0=0$).
- The soil is initially saturated with TCE, so that all sorption sites are filled ($\theta_0=1$).

The following equation is the model governing rapid desorption kinetics from soil:

$$[TCE]_t = \frac{2k_d\left(e^{\sqrt{4k_d(k_a\beta)}t} - 1\right)}{\left(\sqrt{4k_d(k_a\beta)}\right)\left(e^{\sqrt{4k_d(k_a\beta)}t} + 1\right)} \qquad (6)$$

where: [TCE] = gaseous phase concentration of TCE [molecules / cm^3]

t = time

k_a = Rate coefficient for adsorption

k_d = Rate coefficient for desorption

The constant β is defined as: $\beta = -\frac{V}{SAf}$ (7)

where: V = Volume of cell [cm^3]

SA = Surface Area of soil particle [cm^2]

f = number of total sites per unit surface area [# total sites / cm^2]

This equation contains two fit parameters, βk_a, and k_d, which are found by fitting the equation to the experimental data (time and [TCE]). The equation is placed in a curve-fitting software to determine parameters βk_a and k_d and analyze the "goodness of fit" regression results. Results are shown in Chapter 4 and Appendix F.

Optical Measurement of Desorption

TCE concentration is measured in this experiment using an optical apparatus described below. The sample cell is a glass tube, 0.5 inch diameter and 17.1 inches long. Desorption is monitored after contaminated soil is placed in the tube and the ends are sealed. A vacuum is established in the cell to observe TCE desorption without atmospheric interferences. Light passes through the sample cell to a detector, where minute changes in light intensity are measured. When TCE desorbs from a soil sample, it enters the vapor phase in the sample cell. Increasing numbers of TCE molecules freed in the sample cell absorb light passing through the cell, causing the signal reaching the detector to decrease. In this way, changes in the vapor concentration of TCE are measured by changes in the intensity of light hitting the detector. Figure 4 shows a section of the sample cell (of length l) with TCE molecules desorbed from soil. The incident light

intensity (I_o) is decreased to the transmitted intensity (I_t) as TCE molecules absorb infrared light passing through the cell.

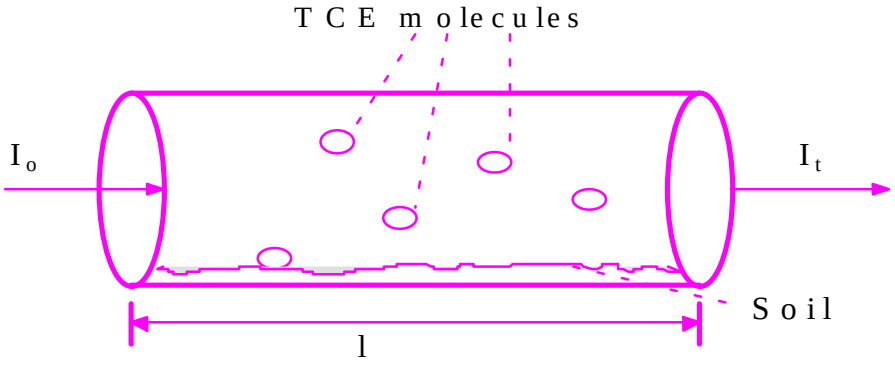

Figure 4. Illustration of Optical Measurement of TCE

The Beer-Lambert Law is used to relate light intensity to TCE concentration. Beer's Law states that as the concentration of an absorbing species increases, the intensity of a ray of light passed through that species decreases exponentially (Sawyer et al., 1994: 390). As desorption occurs in the cell, the TCE concentration increases, and the intensity of light hitting the detector (transmitted intensity) decreases exponentially. This is shown by the following expression:

$$\frac{I_t}{I_o} = e^{-\sigma_{abs} l [TCE]} \qquad (8)$$

where: I_t = Transmitted Intensity [µvolts]

I_o = Incident Intensity [µvolts]

σ_{abs} = cross-section for absorption [cm^2/molecule]

l = path length of cell [cm]

[TCE] = TCE vapor concentration in sample cell [molecules/cm^3]

To use this relationship, the cross section for absorption (σ_{abs}) must be found.

Determination of Cross-Section for Absorption

The cross sectional area for absorption (σ_{abs}) has units of area, and represents the rate at which light is absorbed by the material. This parameter was determined experimentally. TCE vapor was released to the cell and the ambient temperature, cell pressure, and light intensity changes were recorded. Plotting the data as ln (I_t / I_o) vs. [TCE] yields a curve which can be fitted by Beer's Law to determine σ_{abs}. The following paragraphs provide an overview of how σ_{abs} was determined in this experiment. Further explanation and details about the correction formula is included in Appendix B.

First a relationship is established between pressure changes in the cell and TCE concentrations. A vial was attached to the cell for release of TCE vapor into the cell. The cell is drawn down to vacuum, so that the only added pressure will be from TCE vapor. Thus, the concentration of TCE in the cell can be measured by direct measurement of pressure rise and temperature, using the Ideal Gas law:

$$[TCE] = \frac{P}{RT} \qquad (9)$$

where: P = Pressure in cell [torr]

T = Temperature [^oK]

R = Ideal Gas constant = 1.0356×10^{-19} [cm^3-torr / molec-^oK]

[TCE] = Concentration of TCE in the cell [torr]

As the TCE vapor is released to the cell, the cross sectional area for absorption is found by relating light changes to TCE concentration changes. The ln (It/Io) data is plotted against changes in TCE pressure to determine σ_{abs}.

Researchers have shown that in the wavenumber range used in this experiment (3080-3123 cm^{-1}) TCE does not absorb all light frequencies passed through the sample cell. There is a fraction of light that passes through to the detector, unaffected by *any* change in TCE concentration (Fares, 1994; Kindt, 1994; LaPuma, 1994). Thus, a modification must be applied to Beer's Law to account for the unabsorbed light. Research performed using the same bandpass filter and apparatus of this experiment found that Beer's Law can be modified to account for the unabsorbed light. The resulting equation is shown below (Fares, 1994; Kindt, 1994; LaPuma, 1994):

$$I_t = (Ae^{B[TCE]} + (1 - A))I_o \qquad (10)$$

where: A = Correction factor = 29 cm-1 / 43 cm-1

B = $-\sigma_{abs}l/RT$

This modified Beer-Lambert law was curve fit to the data and the constants A, B, and I_o were determined. The cross section for optical absorption is found by multiplying B by (RT/l), according to the following equation:

$$\sigma_{abs} = B\frac{RT}{l} \tag{11}$$

Data used to determine the cross section for absorption is below.

Multiple runs of TCE pressure changes vs. $\ln(I_t/I_o)$ were performed. The value of σ_{abs} used for the duration of desorption runs was determined by averaging the σ_{abs} values found in 7 runs of ([TCE] vs. I_t data). The values of σ_{abs} and the resulting average σ_{abs} value are shown Table 1.

Table 1. Cross Section Absorption Data for TCE

Run Number	σ_{abs} Value	σ_{abs} Std. Deviation
1	3.06 x 10-20	0.023 x 10-20
2	3.51 x 10-20	0.031 x 10-20
3	3.56 x 10-20	0.017 x 10-20
4	3.75 x 10-20	0.025 x 10-20
5	3.50 x 10-20	0.024 x 10-20
6	3.34 x 10-20	0.020 x 10-20
7	3.35 x 10-20	0.024 x 10-20
AVERAGE	**3.44 x 10-20**	**0.063 x 10-20**

The experimentally determined value of σ_{abs} for in this research effort was $3.44 \pm .06 \times 10^{-20}$ cm^2**.** This measurement of σ_{abs} for TCE is slightly higher than a value of $3.34 \pm .01 \times 10^{-20}$ cm^2, reported in similar research (Fares et al., 1995:1566). However, the standard deviation is also slightly larger. Within the reported margins of error (3.38-3.50) x 10^{-20} cm^2 and (3.33-3.35) x 10^{-20} cm^2, the values differ by only 0.03 x 10^{-20} cm^2. The

average cross section for absorption value of $\mathbf{3.44 \pm .06 \times 10^{-20}\ cm^2}$ was used for data analysis in transforming signal intensity to TCE concentration data.

Chapter 3 - The Experiment

Overview of Spectroscopy

The experiment was designed to use infrared spectroscopy to measure TCE concentrations in the sample cell. TCE, being an organic molecule, yields a unique spectra in the mid-infrared region, near a wavelength of $\lambda = 3.2\ \mu m$. Several researchers demonstrated that TCE readily absorbs infrared radiation at 3040 - 3140 cm^{-1} (Fares, 1994: 52-54; Kindt, 1994: 41; LaPuma, 1994: 34-39). A bandpass filter was used to allow light only of this frequency range to pass through to the detector. Any change in TCE concentration in the sample cell was reflected by a change in light intensity on the detector.

Overview of Experiment

Desorption was measured using an optical apparatus for infrared absorption. The contaminated soil was inserted in a glass cell, vacuum was established, and light was passed through the cell to measure TCE desorption from the soil. The experiments were conducted under a vacuum to eliminate atmospheric interference. A computer was used for continuous data acquisition (pressure and light intensity readings). A schematic of the apparatus is shown in Figure 5. A table of specific equipment used in the experiment, including item name, manufacturer, type, and model number for each piece, can be found in Appendix C.

Optical Train Components

The optical train consisted of many components. The following paragraphs explain each component, mentioned in the sequence of the light path.

At the beginning of the light path was the power supply and the infrared source. The infrared beam began in a quartz-halogen 100 watt lamp, mounted in a black cylindrical housing and directed toward the optical train. The power supply delivered 12 volt, 60 hertz to the lamp.

Following the light source was the light shield. A shield of cardboard was used to direct light from the source to the rest of the train and prevent extraneous light from flooding the apparatus. A large circular hole was carved in the shield to allow a beam of light to pass through.

The beam was narrowed and directed through use of an aperture, lens, and mirrors. A flat, black, cylindrical aperture placed about 24 inches from the source narrowed the beam to the lens. A 1 inch diameter, 50 cm focal length, CaF_2 lens was used to focus the beam so it could pass through the narrow glass cell. A flat silver mirror was used to change the direction of the beam and send it into the cell.

Before sending the beam into the sample cell, it was chopped at a specified frequency. A slotted rotating disk inserted in the beam path helped minimize detector noise and allowed distinction of the two beams. The choppers were controlled by chopper controllers set at a specific frequency for each beam. The beam through the sample cell

was chopped at 155 Hz and the reference beam was chopped at 100 Hz. Output from the chopper controllers was sent to the Lock-In Amplifiers as the reference signal.

The sample cell was a glass cylindrical tube with windows on the ends. The ends of the glass cell were fitted with calcium fluoride (CaF_2) windows, mounted at Brewstar's angle. CaF_2 windows close the cell and enable a vacuum to be established, while still allowing the infrared beam to pass. The sample cell was a hollow, 1/2 inch diameter glass tube, 17.1 inches long. It was connected to the glass windows and the vacuum system with 1/2 inch Cajun Tube Fittings. These fittings were made of Type 316 stainless steel and placed on the outside of the glass tubes. When tightened, the fittings pressed Kelvar (teflon) o-rings against the glass, sealing the cell so a vacuum could be established. Teflon o-rings were necessary because they did not absorb TCE as other o-rings did (LaPuma, 1994:54).

A second lens of 1 inch diameter and 5 cm focal length was placed at the end of the sample cell to gather the exiting beam and focus it onto the detector. Addition of this lens to the optical design greatly increased signal reading.

An optical bandpass filter designed to allow frequencies of 3080 - 3123 cm^{-1} to pass was attached to the cap of the detector. (A hole was drilled in the cap to allow the beam to pass.) Placement of the filter just before the detector ensured that no extraneous light would hit the detector. All radiation, except that sent through the cell and readily absorbed by TCE, was filtered out from the beam.

A thermoelectrically cooled, Indium Arsenide detector was used to measure light intensity. The detector was cooled through use of a temperature controller and heat sink assembly. It was imperative to operate the detector at the specified temperature and resistance. Other settings, although improving the signal-to-noise ratio, will likely damage the detector. Specifications for the detector and controller are cited in Appendix C. Advantages of the thermoelectrically cooled detector include a fast response time, minimal output signal in the absence of illumination, and continuous measurement of the beam over long periods of time without the need to refill liquid nitrogen every 6 hours (Skoog and Leary, 1992: 98-99). One detector was used to gather intensities from two beams of light. The total signal was sent to a transimpedance preamplifier for signal gain and then to the Lock-In Amplifiers where the two light signals, sample and background, were separated from each other.

Data Collection Components

The signals from the choppers and the detector were sent to the lock-in amplifiers. Two lock-ins were used. One amplifier was used for the signal through the cell and the second was used for signal from the unattenuated reference beam. In order to determine the magnitude of each of the elements of the detector signal (sample part and unattenuated part) it was necessary to modulate each beam so the combined signal could be separated into its component parts. The choppers for each beam served this purpose. For each lock-in, the signal from the respective chopper was input as a reference signal and signal from the detector was input as analyte signal. The lock-in filtered out from the detector signal only those signals which did not match the frequency of the chopper. Thus, only

the detector signals that are “locked in” to the chopper signal are amplified and delivered as true signal. All other frequencies are rejected by the lock-in. The lock-in is thus able to take a single readout from the detector, separate it into its components (signal from the sample cell and signal from the reference beam), amplify it, average it, and deliver it as voltage to the computer’s data acquisition board.

A 3/4 HP vacuum pump was attached to the end of the apparatus to establish a vacuum environment within the cell. Valves were placed on the apparatus so the cell could be easily turned on or off to the vacuum. A 100 torr Baratron was attached to the sample cell to gather continuous pressure readings within the cell. Pressure measurements were converted to a voltage signal and sent to the data acquisition board for the computer. The observed leak rate of air into the vacuum cell was 0.026 torr/hr.

For data acquisition, voltage outputs from the two barometers and the two lock-ins were sent to the acquisition board. Labwindows® software was installed on the computer and utilized for acquiring data. A Labwindows® program written in C was built for continuous data acquisition. The program allowed the user to specify the data file and path, and time between samples. The computer recorded five pieces of data for each sample: time, pressure of sample cell, pressure of a control cell, intensity of reference beam, and intensity of sample beam. After the runs were finished, data acquired was transferred to another computer and analyzed with SigmaPlot® and TableCurve® software.

Soil Sample

Homogenous soil of uniform size and shape was chosen to yield well-characterized soil for desorption study. Flint clay from the National Institute of Standards (Standard Reference Material 97b) was used for soil samples. Samples were saturated with liquid TCE for 34 days before testing.

Experimental Design Improvement

Multiplex advantage

One significant improvement added to the apparatus to improve the detection capability was the multiplex design of the experiment. The multiplex advantage was achieved through addition of an unattenuated reference beam to the optical path. This reference beam was sent through a different path than the sample beam and read back onto the same detector. Creation of this second beam allowed any drift in source intensity, ambient temperature, and detector drift to be filtered out of the data. To accomplish this, the original beam was split before entering the sample cell. A gold mirror spatially split the beam into 2 parts. The first beam through the sample cell remained unchanged except that about 1/4 of its intensity was lost. The second beam was sent through the air, chopped at a different frequency, and directed back onto the same detector through careful placement of mirrors. The path of the unattenuated reference beam is shown by a dotted line in Figure 5.

The magnitude of each beam was decoded through use of lock-in amplifiers. The detector measured all light hitting its face and sent it to each lock-in. Since each beam

was chopped at a different frequency, the lock-in could match each light signal with its respective chopper signal and filter out all other measurements. Thus, the lock-in was able to decode the one signal from the detector into its component parts.

The computer program for data collection was modified to read two light intensity signals, one from the sample cell, and one from the second, reference beam. Drifts in data are filtered out of the sample beam during data analysis. The transmitted signal, I_t, is divided by the reference signal, I_r, to remove drifts in source intensity, ambient temperature, and detector drift. Chapter 4 presents data measurements with and without the second, reference beam. Any visible improvement in noise reduction from the multiplex design is discussed in Chapters 4 and 5.

Experimental Procedure

To investigate the long-term desorption mechanism, soil must be monitored for contaminant release past the rapid desorption phase of 1-24 hours. A desorption run of at least 70 hours was conducted to observe whether the desorption mechanism continues to release contaminant beyond the rapid phase or not. Flint clay soil was prepared by saturating the particles with TCE in glass containers. Exposure time to contaminant was 34 days, during which TCE adsorbed into the soil matrix.

Following exposure, approximately 2 grams of soil was removed and dried for 1 hour. Soil drying involved evaporation of the TCE-saturated sample until the soil was of a cracked-clay, but still damp, consistency. Soil was dried for two reasons: (1) it was required for insertion and uniform distribution of soil in the narrow sample cell and (2)

removal of quickly-evaporating TCE (contaminant in the free product, liquid phase) allowed the experiment to focus on release of slowly-desorbing TCE (sorbed/entrained phase contaminant which is not released in the first hour of desorption).

Following the drying/evaporation period, the sample of soil was broken apart and inserted into the cell. The insertion tool was a straw with the last 2 inches cut to form a spoon. The straw (with soil on the spoon) was inserted into the cell, and turned 180^{o} to allow the soil to fall to the bottom of the cell. After soil was distributed along the length of the cell, CaF_2 windows were placed on the ends and the valve to the vacuum was opened. When the pressure reached approximately 1 torr (occurred within 10-30 seconds), the valve to the vacuum was closed and data acquisition started immediately. As desorption proceeded, the computer gathered pressure and light intensity data until run completion. Data acquisition by computer and the use of a thermoelectrically cooled detector allowed continuous measurements throughout the desired desorption run time. Detailed procedures for the contamination of soil samples and desorption testing are outlined in Appendix D.

Chapter 4 - Results

Overview

This chapter begins by presenting results pertinent to the first objective of this research effort. Findings from the long term desorption study are presented, and the Langmuir Kinetic model is fit to the desorption data test the assumption of a single type of soil binding site. Fit to long-term data will show if there is a single mechanism affecting contaminant release over the long term or more than one mechanism. Following this determination, a second model is introduced to describe the desorption trend. Subsequently, the desorption data is compared to the profile of a similar experiment. The second research objective is addressed next, showing the utility of this experimental technique to measure desorption. Lastly, the third objective is met by presenting improvements in apparatus design.

Long-Term Desorption

Data collected for the long-term study was imported into SigmaPlot® software for manipulation. Using the concepts described in Chapter 2 (under Optical Measurement of Desorption) the data was transformed from signal intensity to TCE concentration (reported in units of torr). Data transform programs are included in Appendix E. The Langmuir Kinetic model was fit to the data to prove or disprove that a second, slower mechanism exists. Tablecurve® software was used for curve fitting and determination of

parameters. Formulas for curve fit functions and full numerical summaries from Tablecurve® are included in Appendix F.

Figure 6 shows the desorption of TCE from a sample of flint clay (weight: 1.5± 0.2 grams), contaminated in liquid TCE for 34 days. Desorption from the soil was observed for 71 hours. The x-axis shows the duration of the experiment (in hours) and the y-axis shows the change in concentration of TCE in the sample cell (measured in partial pressure of TCE, units of torr). Figure 7 shows the desorption data overlaid by the best fit Langmuir Kinetic Model.

Figure 6. Long-Term Desorption Data Gathered by Infrared Spectroscopy.

Figure 7. Desorption data with Langmuir Kinetic Model fit and overlaid on the data.

Figure 6 shows that the concentration of TCE appears to rise rapidly at first and rise more slowly later. It seems the rate of desorption is fast at first (indicating a rapid desorption phase) and then gradually decreases to a slower rate (a slow desorption phase).

The Langmuir Kinetic Model Fit

As shown in Figure 7, the Langmuir model does not represent the data well. The model first underestimates initial desorption, then overestimates desorption from 8-33 hours. Past 33 hours, the model underestimates the remaining desorption by failing to account for any additional increase in TCE concentration. The Langmuir Kinetic model characterizes the TCE release as reaching a steady-state at approximately 24 hours. As shown in both Figures 6 and 7, the TCE concentration continues to increase well beyond 24 hours, as desorption extends past 70 hours.

The coefficient of determination (r^2 statistic), which measures closeness of fit, is 0.677 for the Langmuir model. This value is well below the optimum of 1.0, further illustrating that the Langmuir is not a good fit. A full printout of the parameters and statistical regression parameters from Tablecurve® is shown in Appendix F.

The lack of fit by the Langmuir model shows that the desorption mechanism is governed by more than one kinetic mechanism controlling the release of contaminant. After 24 hours, (the end of rapid desorption period) a portion of the contaminant still remains within the soil matrix. Release of this portion continues beyond rapid desorption, and TCE does not reach steady-state. Albeit slower than the initial release, desorption of

contaminant continues throughout the data run (well past 24 hours). To adequately describe the slowly desorbing fraction and predict the true release of contaminant, another model describing more than one desorption mechanism must be sought.

The Gamma (Γ) Model

One model that may suitably represent the full desorption trend is the Gamma (Γ) model. Instead of representing the desorption of contaminant using a one-site mechanism (as the Langmuir model does) or a two-site model, the Γ model generalizes the concept of multiple sites for binding to consider a continuum of compartments, ordered by their desorption rate coefficients (Connaughton et al., 1993). The distribution of desorption rate coefficients is assumed to follow a simple, continuous mathematical function. A convenient and flexible model is the gamma density function (Stedinger et al., 1993).

The gamma function of mathematical statistics has been used in research to describe the distribution of pore sizes in soil. Pore size has shown to be an important factor for sorption kinetics (Connaughton et al., 1993). Thus, the relationship between the desorption rate coefficients and a gamma distribution of rate coefficients is plausible. Appendix G shows a more explicit derivation of the Γ model and how it is related to contaminant release.

Assuming a continuum of compartments with a gamma distribution of desorption rate coefficients, the amount of contaminant released after time t is:

$$TCE_t = TCE_\infty \left(1 - \left(\frac{\beta}{\beta + t} \right)^{\alpha} \right) \quad (12)$$

where: $[TCE]_t$ = Concentration of TCE at time t

$[TCE]_\infty$ = Maximum concentration of TCE (reached at equilibrium)

α = shape parameter of the gamma density function

β = scale parameter of the gamma density function

Equation (12) is the governing equation for the Γ model. The mean desorption rate coefficient using the Γ model is simply $k_d = \alpha/\beta$. The Γ model was placed in Tablecurve® and fit to the experimental data. Values for α, β, and $[TCE]_\infty$ were determined by the best fit regression. Figure 8 shows the desorption data with an overlay of the best fit Γ model.

Figure 8. Desorption data with the Γ Model Fit and Overlaid on the data.

As shown by Figure 8, the Γ model fits the desorption data very well, both short-term and long-term. This model seems to account for not only the initial release, but also the release of contaminant *past* the rapid phase of desorption. TCE molecules sequestered in the soil matrix during the rapid phase and released later are well represented by the Γ model in the latter times of 40-70 hours.

Discussion of Curve Fit Results

The Table 2 summarizes the comparison between the one-site Langmuir Kinetic Model and the Γ Model curve fits. (A full printout of curve-fit equations, fit parameters and regression test results for each model is included in Appendix F.)

Table 2. Curve Fit Results

	Langmuir Model	**Γ Model**
Coefficient of Determination (r^2)	0.667 ± 0.073	0.977 ± 0.019
Fit Parameters	$k_d = 0.115 \pm 0.001$ $k_a\beta = 0.176 \pm 0.001$	$\alpha = 0.134 \pm 0.002$ $\beta = 0.268 \pm 0.004$ $TCE_\infty = 1.671 \pm 0.015$ [torr]
Rate Coefficient for Desorption	$k_d = 0.115 \pm 0.001$ [mTorr/s]	$k_d = 0.498 \pm 0.011$ [$hour^{-1}$]

The coefficient of determination (r^2) for the Γ Model is 0.977 -- much better than the Langmuir value of 0.677. This fit indicates the Γ Model is able to well-characterize

the desorption trend throughout the entire 71-hour run. The continually slower increase of TCE over time indicates the desorption mechanism could be based on a continuum of contaminant release sites rather than a single type of site. This idea is demonstrated by the ability of the Γ Model, which is based on a continuous range of desorption rate constants, to fit the data well. The Langmuir Kinetic Model, based on the assumption of a single type of binding site, did not fit the data well, indicating that the long-term desorption mechanism is not based on a single desorption rate.

The fit parameters for the Γ Model (α and β) are parameters for the gamma density function. The density function indicates the likelihood that a randomly selected molecule is in a compartment with a desorption rate coefficient k_d. The constant α is a shape parameter and β is a scale parameter of the gamma density function. (See Appendix G for an illustration and greater detail.) For very small values of α, ($0 < \alpha < 1$) most of the contaminant mass corresponds to very small values of k_d (Connaughton, 1993:2399). The smaller the α, the more contaminant mass located in compartments with small coefficients of desorption. Since $\alpha = 0.134$, (a small fraction), this indicates that most of the mass, and most of the compartments, correspond to very small desorption rate coefficients. Thus, it can be concluded that most of the binding sites in this soil sample possess a small k_d. This suggests 2 items: (1) when sorption experiments are performed over the short term (< 24 hours) slow kinetic compartments may not be identified (2) the contaminant mass, located on those slow kinetic compartments, may be a significant fraction (most) of the total mass, and remain ignored.

The Γ Model described well the changing trend of contaminant release throughout the full desorption mechanism within 71 hours. It fit the data during rapid release and also during slower release, accounting for a slowly desorbing fraction of contaminant. The Langmuir Kinetic Model, which assumed equilibrium and no desorption past the rapid phase of 24 hours, was unable to adequately model desorption over the long term. The Gamma (Γ) Model, however, described both the long-term and short-term desorption mechanisms well, accounting for the slow release of contaminant from interior sites.

Comparison to Similar Experiment

The long-term desorption data gathered in this study is next compared to short-term data gathered on the same apparatus. Fares, Kindt, LaPuma, and Perram studied the desorption of TCE from flint clay over a short-term period of five hours (Fares et al., 1995:1566; Kindt, 1994:61-66). Focus in their study was on the rapid desorption mechanism, and results are shown below in Figure 9. This data is compared to the graph of long-term data from the current study, presented in Figure 6. Both figures show the concentration of TCE on the y-axis in torr and time on the x-axis.

Figure 9. Short-Term Desorption of TCE from Soils
Figure shows desorption from Flint Clay (Δ),
Dolomitic Limestone (O), and Montana soil ( ).
(Fares et al., 1995: 1566)

The TCE desorption from flint clay is represented in Figure 9 by small triangles (it is the lowest of the three curves). The slope of the curve indicates the magnitude of the desorption rate. The most significant difference between the above (short-term) data and the long-term desorption data of Figure 6 is the shape of the curve at the end of the rapid desorption phase. The short-term study has a sharper change (decrease) in slope at about 0.5 hours, while the long-term study has a more gradual decrease in slope over the rang of 0-24 hours. If one focuses on the first five hours of the long-term study, the difference in

slopes is even more pronounced. The contrast in shape can be attributed to different soil sample preparation.

There are two significant differences in sample preparation between the two studies: contamination time and the extent of soil drying. The short-term sample was saturated in liquid TCE for 36 hours, while the long-term sample from the current study was saturated for 814 hours. The time for TCE adsorption into the interior matrix for the long-term study was over 22 times longer than the short-term sample. This may have resulted in more contaminant mass located in slowly-desorbing sites for the long-term sample. This could account for a slow and gradual release of TCE throughout the run time. The short-term sample, with less adsorption time, may have a smaller fraction of slowly desorbing entrained contaminant. This results in increased magnitude of quickly released contaminant in earlier times (increase in the slope of the curve in first hour).

The second difference on sample preparation was the time allowed for soil drying. The extent of soil drying can affect the rate of initial contaminant release. Liquid TCE will release from the surface faster than sorbed TCE, which is bound to the surface of the soil. Wetter soil, with more liquid contaminant, will release that contaminant quicker and establish a higher concentration of contaminant earlier in the sample cell than drier soil. The desorption profile for wet soil will have a higher slope. As visible in Figure 9, the short term sample has a much higher slope initially than the long term sample. The short-term soil sample was dried for 10 minutes and then inserted into the sample cell to measure short-term desorption. The long-term sample, however, was dried for 1 hour, (six times longer) to allow evaporation of most of the liquid TCE. Thus, the initial, rapid

release of liquid contaminant - which would cause a sharp rise the desorption curve - was limited. The long-term desorption study accentuated instead the slowly-desorbing sites. Thus, the desorption curve fot the long-term study is more gradual, focusing on the gradual release of contaminant in latter times.

Advantage of Infrared Spectroscopy

This experiment uses a non-traditional method (for the environmental field) to measure desorption from contaminated soil. Many laboratories use the EPA purge-and-trap method, centrifugation, solvent extraction, or thermal desorption. The EPA method, the most commonly used, can fail to quantify contaminant entrained in the soil matrix. As demonstrated by the long-term desorption data (Figure 6), release of the entrained portion of contaminant has a significant impact on the desorption trend. Ignoring, or failing to quantify this entrained portion will result in poor predictions for contaminant release.

All of the traditional measurement techniques for desorption focus on a single point in time. A desorption profile is found by taking samples at designated time intervals and processing each sample through the test method. Figure 10 shows the data points for two desorption studies. Both studies show the duration of study (in hours) on the x-axis and the amount of contaminant desorption on the y-axis. Note the limited number of sampling points used in each figure to characterize the desorption trend.

Figure 10. Desorption data gathered by Traditional Measurement Techniques.
(Note small number of desorption datum over the range of study.)
Top figure: (Pavlostathis and Jaglal, 1991)
Bottom figure: (Li and Gupta, 1994)

As illustrated by Figure 10, the number of sample points used to characterize the desorption trend is few. The top figure used 10 points over 35 hours while the bottom figure used only 4 over 25 hours. There are two disadvantages to these methods for testing the desorption trend. First, they cannot describe desorption patterns *between* samples. Second, they increase *measurement error* in a desorption trend by drawing new soil samples each time a desorption measurement is made.

Figure 10 shows significant gaps between sample points, thus reducing the fidelity of the model applied to the data. Both studies use less than 11 data points to describe the desorption pattern, and the data are separated by as much as 15 hours. The true desorption trend is unknown between sample times. The existence of these time gaps between sample points leaves a large amount of uncertainty in the actual desorption trend.

The probability of measurement error is increased when a separate test method is run for each sample. This does not lend itself to a robust test technique. Each method contains multiple steps to test a sample for contaminant release, and multiple soil samples to characterize a desorption trend. If one step of the test sequence is varied, it can produce inaccurate data for that sample. Furthermore, when multiple samples are taken, the chance for inaccuracy increases. The number of separate measurements is increased, thus adding to the variance and possibility for measurement error.

The infrared absorption technique used for this research effort is not limited by these disadvantages. The infrared method is able to describe the desorption mechanism *continuously* using a *single* soil sample for each desorption run. Sampling times are

adjustable through the data acquisition program on the computer, and can be reduced to as little as 1 second between sample times. The optical absorption technique used for Figure 7 gathered over 5000 data points during 70 hours. The result is essentially a continuous measurement of desorption. There are no significant gaps in data throughout the experiment. Furthermore, measurement errors in a desorption trend due to different tests for each sample are negated since there is one sample for each desorption run. A single sample is inserted into the sample cell and continuously monitored over time for desorption. No other soil samples are introduced in modeling the desorption trend. The impact of measurement error from multiple samples is significantly reduced when the infrared absorption technique is used.

Optical Design Enhancement

Figure 11 shows the signal readings taken over 27 hours with no TCE in the sample cell (blank concentration). The x-axis shows the duration of data gathering (hours) and the y-axis shows any change in signal intensity. Note that the signal intensity data are normalized (the data column was divided by the average intensity). Normalization enables multiple runs to be compared on the same scale, (i.e. the average signal is always 1). Optimum measurement by the apparatus would show no change in signal intensity (a flat line) since there is no TCE in the cell.

Figure 11. Drift of Signal Intensity over Time.

Figure 11 shows, however, that there is a significant amount of drift in the data. This drift could be from the source intensity, ambient temperature and pressure changes, the detector, the lock-in, or an unidentified cause. The range in signal drift equates to 1.2 % of the average signal value. This equates to a change of 0.24 torr in TCE concentration. (See Appendix H for calculations.) Referring to Figure 6, a data drift of 0.24 torr would dramatically effect the data. The full range of desorption extends only to 0.9 torr over 70 hours. If this drift existed in the desorption data, it could erroneously report a 27% change in the desorption trend. Furthermore, individual, random spikes are present in the data, extending up to 0.6% of the average signal value. These random spikes equate to 0.12 torr of TCE, and could contribute to a 13% error in desorption patterns.

One change in the optical design that reduces the drift in data is addition of an unattenuated reference beam. The creation of a second beam through a multiplex design is described in Chapter 3. The original data are divided by the reference beam data to cancel out any drift in source intensity, ambient temperature, or detector drift. Figure 12 shows the same data run as Figure 11, with an overlay of the resulting signal with a multiplex design.

Figure 12. Drift of Signal Intensity with the Multiplex Design.

The first note of improvement in Figure 12 is that all significant spikes were filtered out of the data. Variation between single data points was about 0.1 % of the total signal, equating to only 0.02 torr of TCE. The second note of improvement is that the data was much flatter. The multiplex design offered a significant improvement by minimizing signal drift. Total drift with the multiplex technique was 3.0 % of the average signal, equating to 0.06 torr of TCE. This reduced the possible error in desorption trends to 6.7% -- a four-fold improvement from prior data. Improvement of the apparatus through a multiplex design greatly improved the ability to accurately quantify minute trends in desorption data.

A primary disadvantage of traditional desorption measurement techniques is the inability of quantify minute increases in desorbed TCE. Thus, many studies falsely report a steady-state desorption pattern after the rapid desorption phase when in reality minute desorption is taking place in the long term. The multiplex apparatus presented in this experiment has the unique ability to characterize the long-term desorption trend. Minute changes in contaminant concentration that remain undetected by traditional test methods are readily measured using infrared absorption spectroscopy.

Chapter 5 - Conclusions and Recommendations

Conclusions

Several conclusions are drawn from this research. The results presented in Chapter 4 provide insight into the long term desorption mechanism; the utility of infrared spectroscopy in measuring continuous desorption; and the effects of apparatus improvements.

The Long-Term Desorption Mechanism

Experiment results show the long-term desorption mechanism does not rely on a single desorption rate. A one-site Langmuir Kinetic Model, based on the assumption of a single type of binding site and a single desorption rate, did not fit the long-term desorption data well. It characterized the TCE concentration as reaching steady-state after 24 hours. In reality, contaminant release extended well beyond 24 hours, continuing through 71 hours. The single-rate Langmuir model could not predict true contaminant behavior -- the release of a slowly desorbing fraction of TCE. Lack of fit by the Langmuir model indicates there is more than one mechanism governing contaminant release. A model with more than one type of binding site and desorption rate is needed to adequately describe the full long-term desorption mechanism.

The Γ Model, incorporating a continuous distribution of desorption rate coefficients, fit the desorption data well. It characterized the changing trend of contaminant release over 71 hours, from rapid to slow contaminant release. This model

identified most of the contaminant in kinetically slow binding sites, and accounted for the slowly desorbing fraction of contaminant.

Results show that a model with more than one type of binding site is needed to adequately describe the slow, long-term desorption mechanism. Interior binding sites may be governed by a second mechanism such as diffusion, which controls slow contaminant release over time. Models based on a two, or three-site desorption mechanism could fit the long-term data and should be investigated. Fit by the Γ Model, which is based on a gamma distribution of desorption rate coefficients, suggests the desorption mechanism could be based on a continuum of release rates. Research into models based on other continuous distribution functions (perhaps the exponential, or power functions) should be investigated.

The ability of the Γ Model to adequately characterize long-term contaminant release is notable. Slow release of entrained contaminant presents one of the greatest challenges in modeling contaminant fate and transport and implementing successful remediation technologies. The ability to predict contaminant release in the slow desorption phase is crucial to predicting fate and transport of contaminants in models. Increasing knowledge and understanding of the slow desorption mechanism is key to developing accurate models, effecting appropriate clean-up technologies, and optimizing the cost, schedule, and performance of environmental project management.

The Advantage of Infrared Spectroscopy

The research demonstrates that infrared absorption spectroscopy is effective for continuous data acquisition in monitoring the long term desorption mechanism. This method is able to measure desorption past the rapid phase and into the slow release phase. Quantification of the entrained portion of contaminant becomes possible with absorption spectroscopy. This desorption test method is advantageous over traditional test techniques. Absorption spectroscopy uses a single soil sample to describe a desorption trend, thereby minimizing the probability for measurement errors. It is able to continuously measure desorption throughout the entire data run.

Apparatus Improvement

Improvement to the optical design of infrared spectroscopy enhances the measurement precision of infrared spectroscopy. Addition of an unattenuated reference beam to the experimental apparatus yielded the multiplex advantage. Drifts in source intensity, ambient temperature, and detector temperature could be filtered out of the data. The multiplex design allowed the capability to measure minute changes in contaminant concentration down to 0.06 Torr of TCE. Applying infrared absorption spectroscopy to long-term desorption measurement is promising.

Recommendations

Several recommendations are suggested to further research of the long-term desorption mechanism and improve the infrared absorption spectroscopy measurement technique.

First, several runs of contaminant desorption are necessary to further validate the findings of this study. The desorption pattern discussed was seen in only two runs of desorption data. Several long-term runs were conducted but much of the data was unusable due to errors in experimental procedures. It is suggested that additional long-term desorption runs be conducted, with longer run times. The observation time should be extended to find if there is a point at which the desorption data levels off asymptotically.

Additional models should be investigated for their ability to describe the desorption process. It has been demonstrated that a one-site model (the Langmuir) is not appropriate while a model of a continuous distribution of binding sites (the Gamma) is. Perhaps there is a two or three-site model which can adequately describe the desorption mechanism. Perhaps there are other continuous distributions, other than the gamma distribution which can characterize long term desorption. Alternative models should be fit to multiple data runs to test their ability to characterize the desorption trend.

With the long-term desorption mechanism validated, several tests could be conducted on the data to determine the effects of different variables on the long-term desorption rate. Variables to test include: competition with water molecules (the effect of soil moisture), contaminant resident time, soil type, and organic content of soil. The effect of these properties on long-term desorption is largely undetermined.

As an improvement to the measurement technique, the sample cell should be modified to allow contaminated soil to be easily inserted into the sample cell. Currently,

the 1/2 inch diameter of the cell restricts the ability to evenly distribute soil along its 17 inch length. The soil tends to form clumps that block the beam of light through the cell, reducing the total signal. These clumps make even soil distribution and a strong signal difficult. A sample cell of 1 or 1 1/2 inch diameter would allow more even distribution of soil samples and lead to less signal loss due to soil blockage.

Lastly, a second modification proposed for the measurement technique is to find a method to allow expeditious transfer of contaminated soil from the contamination jar to the sample cell. This proved to be a major stumbling block in attempting to standardize and replicate desorption runs. The soil, being saturated with contaminant upon removal from the glass jar, often sticks to the straw instead of depositing onto the cell bottom. The soil tends to form clumps that block the beam of light through the cell and reduce the total signal.

To easily insert the soil into the glass cell and gain maximum signal, the soil must be broken up and sufficiently dried/evaporated such that it will readily fall from the insertion tool. However, it must not be dried so much that extensive desorption occurs. Throughout this experiment, differing evaporation times and led to differing amounts of rapid desorption for samples. Samples that were significantly dried and broken up for insertion into the cell showed almost no desorption at all. For some soil runs, it seemed that most of the desorption process had taken place before the sample was even in the cell. The key to the evaporation time is to dry the soil enough so that it does not stick to the insertion tool (the straw), but not so much that significant desorption occurs before the sample is tested. The key to breaking up the soil is to break it enough that it can get into

the cell without blocking significant signal but not so much that all the interior micropores are exposed to the air and long-term desorption becomes irrelevant. Finding an appropriate method of soil insertion into the sample cell will allow standardization and replication of long-term soil desorption runs.

Appendix A - Derivation of the Langmuir Kinetic Model

Relating TCE molecules to sorption sites

The following equations illustrate how any change in the number of TCE molecules results in a direct, linear change in the number of sorption sites available.

Let:
- V = Volume of cell [cm^3]
- SA = a Surface Area of soil particle [cm^2]
- f = number of total sites per unit surface area [# total sites / cm^2]
- θ = fraction of sites occupied by TCE molecules [# sorbed sites / # total sites]
- TCE = gaseous phase concentration of TCE [molecules / cm^3]

If one assumes that one TCE molecule will occupy one soil site, then a decrease in the number of gaseous phase TCE molecules will result in an increase in the number of sorbed soil sites. This is illustrated by the following equation:

$$-\frac{d}{dt}[TCE]V = \frac{d}{dt}(SAf\theta) \tag{13}$$

Equation (13) simplifies to:

$$-\frac{d[TCE]}{dt}V = \frac{d\theta}{dt}SAf \tag{14}$$

The units for each side of Equation (14) are:

[# TCE_g molecules decreasing] = [# additional sorbed sites].

Integrating Equation (14) with respect to time yields:

$$-V(TCE - TCE_o) = SAf(\theta - \theta_o) \quad (15)$$

Where: TCE_0 = Initial gas phase concentration of TCE

θ_0 = Initial fraction of sorbed soil sites

Assuming no gaseous phase TCE initially (TCE_0=0) and solving for θ yields:

$$\theta = \theta_o - \frac{V}{SAf}[TCE] \quad (16)$$

The parameters V, SA, and f are all properties which remain unchanged throughout the desorption process. These can be grouped together into one constant, β. Therefore, if

$$\beta = -\frac{V}{SAf} \quad (7)$$

then Equation (16) reduces to:

$$\theta = \theta_o - \beta[TCE] \quad (17)$$

If TCE is represented by the variable y: $y = [TCE]$

then: $\theta = \theta_o - \beta y$

Now one can substitute y and θ into equation (5):

$$\frac{d[TCE]}{dt} = \frac{dy}{dt} = k_d(\theta_0 - \beta y) - k_a y(1 - \theta_0 - \beta y) \qquad (18)$$

Where: k_d = rate coefficient for desorption

k_a = rate coefficient for adsorption

Integration of Equation (18) yields:

$$\int_0^{[TCE]} \frac{dy}{k_d\theta_0 + (-k_d\beta + k_a - k_a\theta_0)y - k_a\beta y^2} = \int_0^t dt \qquad (19)$$

Let:

$$A = k_a\beta$$
$$B = -k_d\beta + k_a - k_a\theta_0$$
$$C = k_d\theta_0$$

The integral now becomes:

$$\int_0^{[TCE]} \frac{dy}{Ay^2 + By + C} = \int_0^t dt \qquad (20)$$

where the variable of integration is:

$$B^2 - 4AC = k_d{}^2\beta^2 - 2k_a k_d\beta(1 + \theta_0) + k_a{}^2(1 - \theta_0)^2 = \gamma^2$$

The solution of Equation (20) becomes:

$$\frac{1}{\gamma} ln\left(\frac{2Ay + B - \gamma}{2Ay + B + \gamma}\right)\Bigg|_0^{[TCE]} = t \qquad (21)$$

Solving for y yields:

$$y = [TCE]_t = \frac{(B^2 - \gamma^2)(e^{\gamma t} - 1)}{2A\left[(B+\gamma) - (B-\gamma)e^{\gamma t}\right]} \quad (22)$$

Assuming that the soil is initially saturated with TCE (θ_0=1), so that all sites are filled, Equation (22) can be reduced to:

$$[TCE]_t = \frac{2k_d(e^{\gamma t} - 1)}{(B+\gamma) - (B-\gamma)e^{\gamma t}} \quad (23)$$

Since θ_0=1, then $B = -k_d\beta + (1-\theta_0)k_a = k_d\beta + (1-1)k_a = -k_d\beta$

Substituting B in Equation (23) yields:

$$[TCE]_t = \frac{2k_d(e^{\gamma t} - 1)}{(-k_d\beta + \gamma) + (k_d\beta + \gamma)e^{\gamma t}} \quad (24)$$

Equation (24) contains three fit parameters: k_a, k_d, and β. A three parameter fit is not well defined by the experimental data. Fortunately, $k_a\beta$ always appears as a product, reducing the number of adjustable parameters to two. Noting that $k_a >> k_d$, the equation is approximated to:

$$[TCE]_t = \frac{2k_d(e^{\sqrt{4k_d(k_a\beta)}t} - 1)}{(\sqrt{4k_d(k_a\beta)})(e^{\sqrt{4k_d(k_a\beta)}t} + 1)} \quad (6)$$

This equation contains two fit parameters, βk_a, and k_d, which are found using the experimental data. The equation is placed in Tablecurve (a curve-fitting software), and

fitted to the experimental data. The fit parameters and statistical regression results are shown in Chapter 4.

Appendix B - Determination of Absorption Cross Section

The cross section for absorption (σ_{abs}) is needed to relate light intensity changes to TCE concentration. The cross section was determined experimentally using the Ideal Gas law for concentration measurements and then Beer's Law. A correction in the formula for Beer's Law was required due to account for light that is unable to be absorbed by TCE molecules. The following equations show how the cross section was experimentally determined for this research effort.

Relating Cell Pressure to TCE Concentration

First, the TCE concentration was measured in the cell by collecting pressure measurements. The cell began at vacuum and vapor TCE was slowly released into the cell, resulting in a direct change in the cell pressure. The cell pressure rose to about 58 torr (the vapor pressure of TCE at 20^{o}C). Since TCE was the only gas added to the vacuum, the rise in pressure was due only to a rise in TCE concentration. A direct relationship between cell pressure and TCE concentration was made using the Ideal Gas Law:

$$[TCE] = \frac{P}{RT} \tag{9}$$

where: P = Pressure in cell [torr]

R = Ideal Gas Constant [1.0356 x 10^{-19} cm^3-torr / molec-^{o}K]

T = Temperature [^{o}K]

TCE = Concentration of TCE [molecules / cm^3]

Next, the TCE concentration data was added to the light intensity measurements to find the cross section for absorption.

Relating TCE Concentration and Light Intensity

If Beer's Law is used directly, there should be a linear relationship between the TCE concentration changes (i.e. pressure changes) and the natural log of the signal changes:

$$ln\left(\frac{I_t}{I_o}\right) = -\sigma_{abs} l\,[TCE] \tag{8}$$

Substituting Equation (9) into Equation (8) yields:

$$ln\left(\frac{I_t}{I_o}\right) = \frac{-\sigma_{abs} l}{RT} P \tag{25}$$

where: I_t = Transmitted Intensity [μvolts]

I_o = Incident Intensity [μvolts]

σ_{abs} = cross-section for absorption [cm^2/molecule]

l = path length of cell [cm]

[TCE] = TCE vapor concentration in sample cell [molecules/cm^3]

In Equation (25), pressure and light intensity are the only variables. The other parameters (R, T, l, and σ_{abs}) are all fixed. A plot of Equation (25) with P on the x-axis and $\ln(I_t/I_o)$ on the y-axis should yield a straight line whose slope is $(-\sigma_{abs}l/RT)$. The data in this

experiment, however, did not yield a straight line. (See Figure 13.) The data must be corrected to account for lack of linearity.

Correction Formula

A correction is needed because the TCE molecules are unable to absorb all the light frequencies passed by the bandpass filter (Fares, 1994; Kindt, 1994; LaPuma, 1994). The light passed by the bandpass filter falls in the wavenumber range of 3080-3123 cm^{-1}, thus the filter width is approximately 43 cm^{-1}. An absorption scan performed on TCE molecules, however, revealed that TCE molecules absorb only 29 cm^{-1} of the same range of wavenumbers (Fares, 1994; Kindt, 1994; LaPuma, 1994). Thus, the relationship between TCE concentration and light intensity is not direct. There is a fraction of light that will always be transmitted to the detector, regardless of the TCE concentration in the cell. Even at full TCE saturation, some signal will still get through. Thus, a correction factor must be applied to Beer's Law to account for the frequency of light that passes through the cell unaffected by TCE molecules. Research performed using the same bandpass filter and apparatus of this experiment found that the correction can be performed according to the equation (Fares, 1994; Kindt, 1994; LaPuma, 1994):

$$I_t = \left(Ae^{\frac{-\sigma_{abs} l}{RT} P} + (1 - A)\right) I_o \qquad (10)$$

where: A = Correction factor = 29 cm^{-1}/ 43 cm^{-1}

The only changing variables in the above equation are I_t and P_{TCE}. The experimental data (which are I_t and P_{TCE}) were input into Tablecurve® and the equation fitted to it. The

cross section for absorption is found for each run of pressure vs. intensity measurements. The equation placed in Tablecurve® was:

$$y = (Ae^{-B \cdot x} + (1 - A))C \quad (26)$$

where: y = Transmitted Intensity (I_t)

x = TCE concentration (measured in torr)

A = Correction factor = 29 cm-1 / 43 cm-1

B = $-\sigma_{abs} l/RT$

C = Incident Intensity (I_o)

The constants A, B, and C were determined by curve fitting the data to the equation. Figure 12 shows a sample run of pressure and intensity data fit with the above equation. The fit parameters A, B, and C are shown on the printout below.

Figure 13. Curve Fit to Determine Cross Section for Absorption

Determination of Cross Section for Absorption

The cross section is found by simply multiplying the parameter B by (RT/l), according to the following equation introduced in Chapter 2:

$$\sigma_{abs} = B\frac{RT}{l} \tag{11}$$

Multiple runs of TCE pressure changes vs. $\ln(I_t/I_o)$ were performed. The value of σ_{abs} used for the duration of desorption runs was determined by averaging the σ_{abs} values found in 7 runs of (P vs. I_t data). The data of σ_{abs} averaged to yield an overall σ_{abs} value are shown Table 1 in Chapter 2. The average value of σ_{abs} used in this experiment to gather desorption was **$3.44 \pm .06 \times 10^{-20}$ cm^2.**

Appendix C - Experiment Equipment and Specifications

Table 3. Experimental Equipment

Item	Manufacturer	Type	Model
Power Supply	Oriel	12 volt-60 Hz	6393
Lamp Housing	Oriel	Black cylindrical	6358
Halogen Lamp	USHIO	12 volt-100 watt	FCR
Lens	Oriel	50 cm CaF_2	43190
Chopper Controller	Stanford Research, Inc	0-10 VDC	SR 540
Lens	Oriel	5 cm CaF_2	43150
Bandpass Filter	Barr Associates	3040-3140 cm^{-1}	N/A
Detector	Judson EG&G	Indium Arsenide	J12-TE2
Heat Sink	Judson EG&G	N/A	HSA 2
Temperature Controller	Judson EG&G	N/A	TC5
Preamplifier	Judson EG&G	+/- 12 V	RO2M
Lock-in Amplifier	Stanford Research, Inc.	N/A	SR 510
Baratron	MKS Instruments, Inc	122A	00100AD
Vacuum Pump	Franklin Electric	3/4 HP	1091045400
Data Acquisition Board	Phoenix Contact	16 bit analog-to-digital	AT-MIO-16F-5
Computer	IBM	386SX	SM1

Specifications for Experiment Equipment

Detector

Controller should be set at (for -40°C Detector temperature):

- Thermistor Resistance = 19.6 kΩ. Thus TC Temperature Set on the from panel should be set at **19.8**.
- Cooler Current = .7 Amps. Thus TC Current Max Set should be set at **.7**.

Lock-in

The Stanford Lock-in was set at the following settings throughout this experiment. Each setting is marked by an underline:

- Signal Filters - all in out position
- Signal Inputs - cable input from detector went into slot A
- Sensitivity - (varied) but usually set at 50 μVolts.
- DYNAMIC RESOLUTION - low
- Status - none
- Display - X
- Output - cable to computer data acquisition board
- Expand - x1
- Rel - off
- Offset - off
- Time Constant - Pre: varied (usually set at 30 sec for a desorption run)
  - Post: none
- Reference - input cable from chopper controllers, f, square signal, angles vary.

Appendix D - Procedures

Sample Preparation

Contamination of Soil Sample

1. Place soil to be contaminated in glass container and weigh.
2. Add TCE to wet all soil and completely saturate soil in liquid TCE.
3. Place cap on glass container.
4. Allow contaminant to adsorb for 2-45 days
5. Monitor soil daily to ensure TCE has not evaporated. If it has, add more liquid TCE.

Testing of Desorption from Soil Sample

1. Spoon soil out of supernatant into glass beaker and weigh. Add wet soil to beaker until approximately 2.5 grams of soil+TCE is in beaker. Allow liquid TCE to evaporate off sample (about 1 hour needed).
2. Break apart soil, place on straw, insert in sample cell, and turn 180º to allow soil to fall onto cell bottom. Repeat until all of soil sample is placed in cell.
3. Clean off excess soil from end of cell fittings and insert CaF_2 windows on the end. Tighten fittings to seal cell for vacuum.
4. Turn on pump and draw out air until pressure in cell reaches 1-5 torr.
5. Close valve to pump and start data acquisition immediately.
6. Allow computer to acquire data continuously until run is complete.

Data Acquisition

Program for collection of data from apparatus

The following program was written to collect time, pressure, and signal intensity data for this experiment. The program, named pressu4b.c, was written in the C language and is compatible with Labwindows® data acquisition software.

Four data entries were read into the computer: voltsin0 (sample cell pressure); voltsin8 (empty cell pressure - not used in this experiment); voltsin1 (reference signal intensity); and voltsin9 (sample signal intensity). The sampling time for each experiment was reset for each program run. Pressure and signal intensity for the sample cell were plotted on a strip chart during data acquisition.

PRESSU4B.C

```
#include "C:\LW\INCLUDE\formatio.h"
#include "C:\LW\INCLUDE\lwsystem.h"
#include "C:\LW\INCLUDE\userint.h"
#include "C:\LW\INCLUDE\dataacq.h"
/*= INCLUDES
============================================================*/
/*                                                          */
/*  Remember, never modify the contents of include files generated by the  */
/*  User Interface Editor.                                  */
/*============================================================================
======*/
#include "volts1c.h"
/*#include "setup.h"*/
```

```
/*= STATIC VARIABLE DECLARATIONS
==========================================*/

static int panelHandle[1];
static int eventPanelID[1];
static int eventControl[1];
static int loopDoneFlag[1];
static int menuBarHandle;

/*= Defines
============================================================*/

#define TRUE 1
#define FALSE 0

/*= MAIN PROGRAM
==========================================================*/

main()
   {
   /* Declare Variables*/
   int err, start, board_code, file_hndl, rate, i, j, k;
   double voltsin0, voltsin0add, voltsin0avg, voltsinarray[2], wavelen, mark;
   double interval, voltsin8, voltsin8add, voltsin8avg, sttime, stoptime;
   double writtime, voltsin1, voltsin9, voltsin1avg, voltsin9avg;
   double voltsin1add, voltsin9add, sampintnum, voltsinarray2[2];
   char filename[31], sampint[21];

   err = PromptPopup ("Enter Data File Path and Name", filename, 30);
   err = PromptPopup ("Enter the sample intervals in seconds", sampint, 20);
   Fmt(&sampintnum, "%f<%s", sampint);


   file_hndl = OpenFile (filename, 2, 0, 1);
   err = CloseFile (file_hndl);
   panelHandle[VOLTSPAN] = LoadPanel ("volts1c.uir", VOLTSPAN);
   DisplayPanel (panelHandle[VOLTSPAN]);
   SetAxisRange (panelHandle[VOLTSPAN], VOLTSPAN_VOLTS, 0, 0.0, sampintnum, -1, 0.0,
1);
   SetAxisRange (panelHandle[VOLTSPAN], VOLTSPAN_INT, 0, 0.0, sampintnum, -1, 0.0,
50);


   start = FALSE;      /* Initialize Variables and DAQ Board */
   i = 0;
   j = 0;
   Init_DA_Brds (1, &board_code);
```

```
AI_Configure (1, -1, 1, 10, 1, 0);

while (TRUE)       /* Start DAQ Loop */
   {
   /* Read Control Buttons*/
   GetUserEvent (0, &eventPanelID[0], &eventControl[0]);
   switch (eventControl[0])
      {

      case VOLTSPAN_START:    /* Start the Strip Chart */

         start = TRUE;
         SetInputMode (panelHandle[VOLTSPAN], VOLTSPAN_START, 0);
         SetInputMode (panelHandle[VOLTSPAN], VOLTSPAN_STOP, 1);
         SetActiveCtrl (VOLTSPAN_STOP);
         break;

      case VOLTSPAN_STOP:     /* Stop the Strip Chart */

         start = FALSE;
         SetInputMode (panelHandle[VOLTSPAN], VOLTSPAN_START, 1);
         SetInputMode (panelHandle[VOLTSPAN], VOLTSPAN_STOP, 0);
         SetActiveCtrl (VOLTSPAN_START);
         break;

      case VOLTSPAN_RESET:   /* Reset the Strip Chart */

         ClearStripChart (panelHandle[VOLTSPAN], VOLTSPAN);
         start = FALSE;
         SetInputMode (panelHandle[VOLTSPAN], VOLTSPAN_START, 1);
         SetInputMode (panelHandle[VOLTSPAN], VOLTSPAN_STOP, 0);
         break;


      case VOLTSPAN_QUIT:     /* Exit the Strip Chart */

         return;
         break;
      }

      if (start)
         {
         mark = timer();
         interval = sampintnum - .05;
         voltsin0add = 0;
         voltsin8add = 0;
         voltsin1add = 0;
```

```
            voltsin9add = 0;
            sttime = Timer ();
            for (j=0;j<100;j++)
                {
               err = AI_VRead (1, 0, 1, &voltsin0);
               err = AI_VRead (1, 8, 1, &voltsin8);
               err = AI_VRead (1, 1, 1, &voltsin1);
               err = AI_VRead (1, 9, 1, &voltsin9);
               voltsin0add += voltsin0;
               voltsin8add += voltsin8;
               voltsin1add += voltsin1;
               voltsin9add += voltsin9;
                }
            voltsin0avg = voltsin0add/10;
            voltsin8avg = voltsin8add/10;
            voltsin1avg = voltsin1add/100;
            voltsin9avg = voltsin9add/100;
            voltsinarray[0] = voltsin0avg;
            voltsinarray[1] = voltsin8avg;
            voltsinarray2[0] = voltsin1avg;
            voltsinarray2[1] = voltsin9avg;
            PlotStripChart (panelHandle[VOLTSPAN], VOLTSPAN_VOLTS, voltsinarray, 2, 0,
0, 4);
            PlotStripChart (panelHandle[VOLTSPAN], VOLTSPAN_INT, voltsinarray2, 2, 0, 0,
4);
            file_hndl = OpenFile (filename, 2, 1, 1);
            err = FmtFile (file_hndl, "%s<%f    ", sttime);
            err = FmtFile (file_hndl, "%s<%f    ", voltsinarray[0]);
            err = FmtFile (file_hndl, "%s<%f    ",voltsinarray[1]);
            err = FmtFile (file_hndl, "%s<%f    ",voltsinarray2[0]);
            err = FmtFile (file_hndl, "%s<%f\n",voltsinarray2[1]);
            err = CloseFile (file_hndl);
            SyncWait (mark, interval);
            i++;
             }
       }

    }
```

Appendix E - Data Manipulation

SigmaPlot® Transformation Programs

The following transformation programs were written to transfer the signal data to TCE concentration measurements for each sample point.

Time manipulation

This program (titled: time.xfm) changed the time (recorded each day in seconds into column 1) to continuous hours from the start of data acquisition (put into column 3).

```
---------------------------------------------------------------------------------
jsv5D
a=cell(1,1)
s=size(col(1))
x=col(1)-a
put x into col(2)
y=(x)/3600
put y into col(3)
for i=2 to s do
  n=cell(1,i)
  m=cell(1,i-1)
  if (n<m) then
    c=(col(2,i,s)+86400)
    put c into col(2,i,s)
    z=c/3600
    put z into col(3,i,s)
  end if
end for
---------------------------------------------------------------------------------
```

Determination of TCE concentration

The second program (titled: tce-data.xfm) accomplishes 3 tasks. First, for multiplexing, it takes the signal data (column 4), filters out the unattenuated reference beam signal (column 3) and saves it in col 5. Second, it normalizes the data (divides each column by its average) and saves it in columns 6-8. Third, it finds a TCE concentration for each filtered signal measurement (saves it into column 10).

```
jsv5D
itio=col(4)/col(3)
put itio into col(5)
ionorm=col(3)/mean(col(3))
itnorm=col(4)/mean(col(4))
itionorm=col(5)/mean(col(5))
put ionorm into col(6)
put itnorm into col(7)
put itionorm into col(8)
R=1.0356*10^(-19)
T=292.8
abs=3.44*10^(-20)
len=43.5
max=cell(5,1)
dat=-ln(col(5)/max)
pTCE=dat*R*T/(abs*len)
put pTCE into col(10)
```

Appendix F - Curve Fit and Regression Results

Curve-Fitting Functions

The following functions were placed in Tablecurve® as User Functions and fit to the experimental data to determine fit parameters. A full printout of fit parameters and regression results is noted for each equation fitted to experimental data.

Determination of σ_{abs}

The following formula, Beer's Law with a correction factor, was used to find σ_{abs}.

$$y = (ae^{-bx} + (1-a))c \qquad (10)$$

where: y = Transmitted signal intensity data

x = Pressure data

a = constant to account for signal that cannot be blocked by TCE

b = σ_{abs}l / RT = constant multiple of σ_{abs} .

c = Incident signal intensity (average)

The constant b was multiplied by (RT/l) to yield a σ_{abs} for that data run. A sample printout of fit parameters for σ_{abs} is included in Appendix B.

Langmuir Kinetic Model

Equation 6 from chapter 2 was placed in Tablecurve® with the following notation:

$$y = 2a\,(e^{\,sqrt\,(4ab)\,x} - 1) \,/\, [(sqrt(4ab)(e^{\,sqrt\,(4ab)\,x} + 1)] \qquad (27)$$

where: y = TCE concentration [molecules/cm^3]

x = time [hours]

a = k_d = rate coefficient for desorption

b = βk_a = constant x rate coefficient for adsorption

The rate coefficient for desorption was simply parameter a. A printout of fit parameters, statistical regression results, and errors for the Langmuir model is shown at the end of this Appendix.

Γ Model

Appendix G shows the derivation of the Γ model. The governing equation for this model is Equation (28), shown at the end of Appendix G. This equation was placed in Tablecurve® to determine the parameters for a best-fit curve and the resulting regression statistics. The formula used in the User Function is:

$$y = (1 - (a/(a+x))^b)c \qquad (28)$$

where: y = TCE concentration at time x [molecules/cm^3]

x = time [hours]

a = β = (scale) fit parameter for the Γ model

b = α = (shape) fit parameter for the Γ model

c = maximum TCE concentration (reached at equilibrium)

The desorption rate coefficient is found by combining parameters a and b: $k_d = b/a$. A printout of fit parameters, statistical regression results, and errors for the Γ model is shown below.

Fit Parameter and Regression Results

The following figures include the fit parameters for each model above (Langmuir and Gamma) with statistical regression results also included.

Figure 14. Fit Parameters for the Langmuir Kinetic Model

Figure 15. Fit Parameters for the Gamma Model

Appendix G - Derivation of the Gamma (Γ) Model

Background (Connaughton et al., 1993)

The Gamma Model, referred to in this research by its Greek symbol, Γ, is a method postulated to describe long-term desorption data. It is different from the Langmuir model in that instead of assuming all soil sites contain the same desorption rate coefficient, it recognizes that different natural soil particles contain different sorptive compartments. Each compartment contains its own physical constraints on contaminant release -- its own k_d. Thus, there exists a mixture of rate constants for a given mass of soil. The compartments are considered to be continuum of sites, ordered by their desorption rate constants.

If one defines: k = desorption rate coefficient

f(k) = likelihood that a randomly selected molecule is in a compartment with desorption rate coefficient k

= probability density function for the coefficient k

then the sum of all probabilities for the different k values will be one:

$$\int_0^\infty f(k)dk = 1 \qquad (29)$$

One can assume that f(k) is described by a simple unimodal and continuous mathematical function. A convenient and flexible model is the gamma density function, or gamma distribution:

$$f(k) = \frac{\beta^{\alpha}}{\Gamma(\alpha)} k^{\alpha-1} e^{-\beta k} \tag{30}$$

where: f(k) = gamma density function, or gamma distribution

$\Gamma(\alpha)$ = gamma function of mathematical statistics (see below)

β = scale parameter (stretch or compresses f(k) horizontally: $\beta>0$)

α = shape parameter of the gamma density function ($\alpha>0$)

The gamma density function is a probability function in which the variable of interest (in this case k) has a skewed distribution. With the gamma distribution, the mean desorption rate constant is $k = \alpha/\beta$, and the standard deviation of the desorption rate constant is $\sigma_\kappa = (\alpha)^{1/2}\beta$.

The gamma function of mathematical statistics (different from the gamma *density* function) is defined by:

$$\Gamma(\alpha) = \int_0^{\infty} k^{\alpha-1} e^{-k} dk \tag{31}$$

The gamma function has been used in research to describe the distribution of pore sizes in soil. Also, pore size has shown to be an important factor for sorption kinetics. Thus, the relationship between the desorption rate coefficients and the gamma distribution is plausible.

Figure 16 shows various plots of the gamma density function. The x-axis shows the range of desorption rate constants, k, and the y-axis shows the probability of a soil site

having that rate coefficient. The effect of α on the distribution of rate coefficients is drawn.

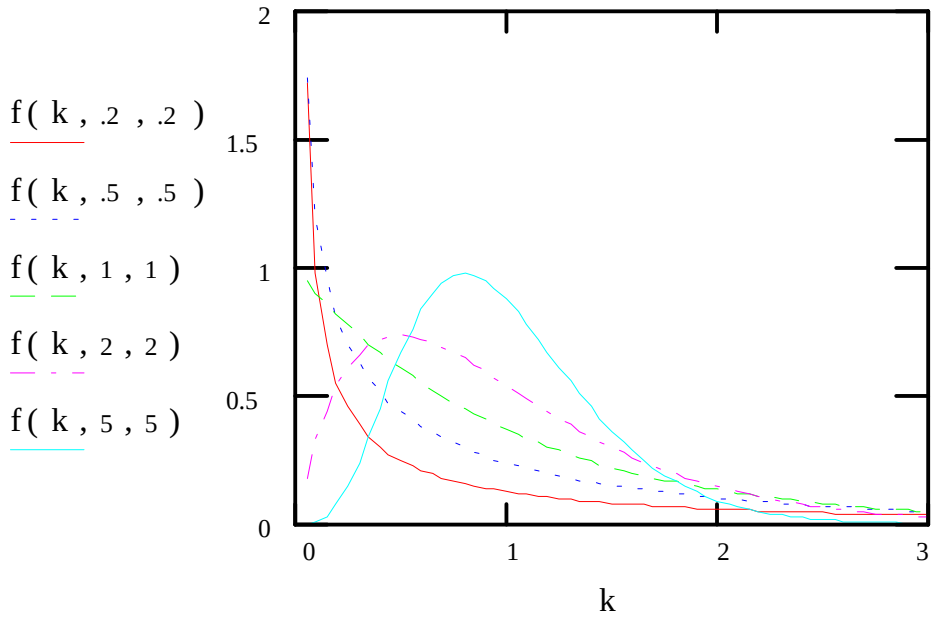

Figure 16. Curves of the Gamma density function. Shows the effect of α on the distribution of k

In the above figure: k = desorption rate coefficients

f(k,α,β) = gamma distribution, Equation (30):

$$f(k,\alpha,\beta) := \frac{\beta^{\alpha}}{\Gamma(\alpha)} \cdot k^{\alpha-1} \cdot e^{-\beta \cdot k} \qquad (30)$$

Each curve f(k) shows the distribution of contaminant throughout the range of desorption rate coefficients. When $0 < \alpha < 1$, the curve is highly skewed to the left, as shown by curves f(k,.2,.2) and f(k,.5,.5). Most of the soil has very small values of k. When α=1, shown by the curve f(k,1,1), the distribution is exponential. Most of the

contaminant mass is still located in compartments with very small values of k. As α increases beyond 1, the distribution becomes increasingly symmetric with small values of k occurring less frequently.

Relating the Γ *model to contaminant release*

The primary interest in the study of desorption is the fraction of mass located in compartments with very small values of k, since this mass will be released very slowly. Thus, the desorption rate distribution when $\alpha<1$ is of primary interest. The release rate from soil with this distribution can be computed analytically.

The fraction of mass with desorption rate constant k, remaining sorbed after time t is e^{-kt}. The total mass remaining sorbed to soil after time t is

$$M(t) = \int_0^\infty Mf(k)e^{-kt}dk = M\left(\frac{\beta}{\beta + t}\right)^\alpha \tag{32}$$

where M = total initial sorbed contaminant mass (at equilibrium)

M(t) = total sorbed contaminant mass after time t

The fraction of contaminant *released* after time t is

$$F(t) = 1 - \frac{M(t)}{M} = 1 - \left(\frac{\beta}{\beta + t}\right)^\alpha \tag{33}$$

where: F(t) = fraction of total contaminant mass released through time t

The fraction of total contaminant desorbed can also be represented by the *concentration* of released contaminant, according to the following equation:

$$F(t) = \frac{TCE_t}{TCE_\infty} = \left(1 - \left(\frac{\beta}{\beta + t}\right)^{\alpha}\right) \tag{34}$$

where: TCE_t = Concentration of contaminant (TCE) at time t

TCE_∞ = Maximum concentration of contaminant (TCE)
= concentration at equilibrium

Application of the Γ model to this experiment

The gamma model can be applied to the data in this research effort by arranging Equation (34) to determine the concentration of TCE at any time t. Solving for TCE_t in the above equation:

$$TCE_t = TCE_\infty \left(1 - \left(\frac{\beta}{\beta + t}\right)^{\alpha}\right) \tag{28}$$

where: TCE_t = concentration of TCE measured in the sample cell at time t

TCE_∞ = maximum concentration of TCE (reached at equilibrium)

This is the governing equation for the Γ model in this research experiment. The data for TCE_t and t were imported into Tablecurve® and the Γ model was fit to the experimental data. The parameters α, β, and TCE_∞ were determined by the best fit curve. A summary

table of coefficients for the Γ Model is in included in Chapter 4, and a printout of fit parameters and regression results is shown in Appendix F.

Appendix H - Signal Improvement Calculations

The following equations show how the percent (%) signal drift, change in TCE concentration, and percent desorption change were calculated before and after multiplexing.

Percent Signal Drift

Each run of data had some drift in the signal intensity over time. This was measured in % signal drift, equating to the % of average total signal shown to be drifting. Since the drift data was normalized, the total signal always averages to 1.000. The following formula is used to calculate the amount of signal drift:

% drift = [(maximum signal - minimum signal) / average signal] x 100% (36)

The maximum signal is the highest point of signal intensity in the data run and the minimum signal is the lowest point. The average signal for normalized data is 1.000. Computations from each case, before and after multiplexing are shown below.

Before Multiplexing:

$$\% \text{ drift} = [(1.005 - 0.993) / 1.000] \times 100\%$$

$$= [0.012 / 1.000] \times 100$$

$$= 1.2\ \%$$

After Multiplexing:

$$\% \text{ drift} = [(1.001 - 0.998) / 1.000] \times 100\%$$

$$= [0.003 / 1.000] \times 100$$

$$= 0.3\ \%$$

TCE Concentration Drift

The data for TCE concentration was deducted from signal measurements. When a drift exists in the intensity data, then a resulting drift in TCE concentration will also occur. The TCE concentration drift is measured in torr (the same units used to quantify desorption). To relate intensity drift to TCE concentration drift, Beer's law is used.

$$\mathbf{[TCE]\ drift = \ln(\Delta It/Io)\ RT/\ \sigma_{abs} l} \qquad (37)$$

where: [TCE] = Concentration of TCE measured in torr

ΔIt = (% Signal Drift x Mean signal intensity) + Mean Intensity

Io = Mean Signal Intensity = 50.34 μVolts

R = Gas Constant = 1.0356×10^{-19}

T = ambient temperature during run = 294^{o}K

σ_{abs} = cross section for absorption = 3.44×10^{-20} cm^{2}

l = cell length 43.5 cm^{-1}

Before Multiplexing:

[TCE] drift = $\ln(\Delta It/Io)\ RT/\ \sigma_{abs}l$

$= \ln((.012*50.34 + 50.34)/50.34)*1.0356x10^{-19}*294\ /(3.44x10^{-20}*43.5)$

= 0.24 torr

After Multiplexing:

[TCE] drift = $\ln(\Delta It/Io)\ RT/\ \sigma_{abs}l$

$= \ln((0.003*50.34 + 50.34)/50.34)*1.0356x10^{-19}*294\ /(3.44x10^{-20}*43.5)$

= 0.06 torr

Desorption Trend Impact

Any drift in signal data and TCE concentration will result in a possible drift in desorption data. The total desorption trend examined in this thesis reached over the range of 0 to 0.90 torr. This is a narrow span of concentration change, thus any drift in TCE concentration measurements could significantly affect the desorption trend. The following formula is used to quantify the impact of signal/concentration drift on the desorption trend:

% drift in desorption trend = [TCE] drift / total Δ in [TCE]) x 100% (38)

where: [TCE] drift = drift TCE concentration determined above

total Δ in [TCE] = maximum range of TCE concentrations observed during desorption experiment

= $[TCE]_{max}$ - $[TCE]_{min}$ observed from Figure 6.

= 0.90 torr - 0.0 torr = .90 torr

Before Multiplexing:

% drift in desorption trend = (0.24 torr / 0.90 torr) x 100%

= 27 %

After Multiplexing:

% drift in desorption trend = (0.06 torr / 0.90 torr) x 100%

= 6.7 %

Bibliography

Avon, Lizanne and John D. Bredehoeft. "An Analysis of Trichloroethylene Movement in Groundwater at Castle Air Force Base, California," Journal of Hydrology, 110: 23-50 (January 1989).

Ball, William P. and Paul V. Roberts. "Long-Term Sorption of Halogenated Organic Chemicals by Aquifer Material. 2. Intraparticle Diffusion," Environmental Science and Technology, Vol. 25 No 7: 1237-1249 (1991).

Bourg, Alain C. M., Christophe Mouvet, and David N. Lerner. "A review of the Attenuation of Trichloroethylene in Soils and Aquifers," Journal of Engineering Geology, 25: 359-370 (November 1992).

Cho, H. Jean, Peter R. Jaffe, and James A. Smith. "Simulating the Volatilization of Solvents in Unsaturated Soils During Laboratory and Field Infiltration Experiments, Water Resources Research, Vol. 29 No 10: 3329-3342 (October 1993).

Connaughton, Doreen F., and others. "Description of Time-Varying Desorption Kinetics: Release of Naphthalene from Contaminated Soils," Environmental Science and Technology, Vol. 27 No 12: 2397-2403 (1993).

Crotwell, Amelia, and others. An Evaluation of Vapor Extraction of Vadose Zone Contamination. Contract No. DE-ACO5-840R21400. Oak Ridge Tennessee: Oak Ridge National Laboratory, May 1992.

Downey, Douglas C and Michael G. Elliott. "Performance of Selected In Situ Soil Decontamination Technologies: An Air Force Perspective," Environmental Progress, Vol. 9 No 3: 169-173 (August, 1990).

Estes, Thomas J., Rajiv V. Shah, and Vincent L. Vilker. "Adsorption of Low Molecular Weight Hydrocarbons by Montmorillonite," Environmental Science and Technology, Vol. 22 No 4: 377-381 (1988).

Fares, Abdellatif. Use of Infrared Spectroscopy to Determine the Effect of Temperature on the Desorption Rates of Trichloroethylene from Plastic Clay 98b. MS thesis, AFIT/GEE/ENP/94S-01. School of Engineering, Air Force Institute of Technology (AU), Wright-Patterson AFB OH, September 1994.

Fares, Abdellatif, Benjamin T. Kindt, Peter LaPuma and Glenn P. Perram. "Desorption Kinetics of Trichloroethylene from Powdered Soils," Environmental Science and Technology, Vol. 29: 1564-1568 (1995).

Farrell, James and Martin Reinhard. "Desorption of Halogenated Organics from Model Solids, Sediments, and Soil under Unsaturated Conditions. 2. Kinetics, Environmental Science and Technology, Vol. 28 No 1: 63-72 (1994).

Government of Canada. Priority Substances List Assessment Report on Trichloroethylene. Canadian Environmental Assessment Report. Ottowa, Canada: Minister of Supply and Services, 1993.

Grathwohl, Peter and Martin Reinhard. "Desorption of Trichloroethylene in Aquifer Material: Rate Limitation at the Grain Scale," Environmental Science and Technology, Vol. 27 No 12: 2360-2366 (1993).

Hylton, T. D. "Evaluation of the TCE Catalytic Oxidation Unit at Wurtsmith Air Force Base," Environmental Progress, 11: 54-57 (February 1992).

Kindt, Benjamin T. Experiment Using Infrared Spectroscopy to Study the Effect of Soil Characteristics upon the Rate of Trichloroethylene Desorption. MS thesis, AFIT/GEE/ENP/94S-02. School of Engineering, Air Force Institute of Technology (AU), Wright-Patterson AFB OH, September 1994.

Kreamer, David K., and others. "Vapor Adsorption of Trichloroethylene on Quartz Sands of Varying Grain Size," Journal of Environmental Engineering, Vol. 120 No 2: 348-359 (March/April 1994).

LaPuma, Peter. Use of Infrared Spectroscopy to Determine the Effect of Resident Time on Desorption Rate from Flint Clay. MS thesis, AFIT/GEE/ENP/94S-03. School of Engineering, Air Force Institute of Technology (AU), Wright-Patterson AFB OH, September 1994.

Li, Yuncong and Gian Gupta. "Adsorption/Desorption of Toluene on Clay Minerals," Journal of Soil Contamination, Vol. 3 No 2: 127-135 (1994).

Mackay, Douglas M. and John A. Cherry. "Groundwater Contamination: Pump and Treat Remediation," Environmental Science and Technology, Vol. 23 No 6: 630-636 (June 1989).

Morel, Francios M. M. and Janet G. Hering. Principles and Applications of Aquatic Chemistry. New York: John Wiley and Sons, Inc., 1993.

Ong, Say Kee and Leonard W. Lion. "Mechanisms for Trichloroethylene Vapor Sorption onto Soil Minerals," Journal of Environmental Quality, Vol. 20: 180-188 (1991).

Ong, Say Kee and Leonard W. Lion. "Trichloroethylene Vapor Sorption onto Soil Minerals," Soil Science Society of America Journal, Vol. 55: 1559-1568 (1991).

Pavlostathis, Spyros G. and Kendrick Jaglal. "Desorptive Behavior of Trichloroethylene in Contaminated Soil," Environmental Science and Technology, Vol. 25 No 2: 274-279 (1991).

Pavlostathis, Spyros G. and Geeyerpurnam N. Mathavan. "Desorption Kinetics of Selected Volatile Organic Compounds from Field Contaminated Soils," Environmental Science and Technology, Vol. 26 No 2: 532-538 (1992).

Perram, Glen P. Class Lecture, OENG 799, The Kinetic Mechanism of Desorption. School of Engineering, Air Force Institute of Technology, Wright-Patterson AFB, OH, February 1995.

Pignatello, J. J. "Sorption Dynamics of Organic Compounds in Soils and Sediments," Reactions and Movements of Organic Chemicals in Soils (SSSA special publication; no. 22). 45-80. Madison, WI: Soil Society of America, Inc. 1989.

Reeder, Major Thomas L. Vadose Zone Contamination Measurements and Modeling. MS thesis, AFIT/GEE/ENV/93S-13. School of Engineering, Air Force Institute of Technology (AU), Wright-Patterson AFB OH, September 1993.

Sawhney, B. L., J. J. Pignatello, and S. M. Steinberg. "Determination of 1,2-Dibromoethane (EDB) in Field Soils: Implications for Volatile Organic Compounds," Journal of Environmental Quality, Vol. 17: 149-152 (1988).

Sawyer, Clair N., Perry L. McCarty and Gene F. Parkin. Chemistry for Environmental Engineering (Fourth Edition). New York: McGraw-Hill, Inc., 1994.

Schaumburg, Frank D. "Banning Trichloroethylene: Responsible Reaction or Overkill?" Environmental Science and Technology, Vol. 24 No 1: 17-22 (January 1990).

Schwille, Friedrich. Dense Chlorinated Solvents in Porous and Fractured Media. Chelsea, MI: Lewis Publishers, Inc., 1988.

Siegrist, Robert L. "Volatile Organic Compounds in Contaminated Soils: The Nature and Validity of the Measurement Process," Journal of Hazardous Materials, Vol. 29: 3-15 (1992).

Skoog, Douglas A. and James J. Leary. Principles of Instrumental Analysis. Fort Worth: Saunders College Publishing, 1992.

Smith, James A. and others. "Effect of Soil Moisture on the Sorption of Trichloroethylene Vapor to Vadose-Zone Soil at Picatinny Arsenal, New Jersey" Environmental Science and Technology, Vol. 24 No 5: 676-683 (1990).

Stimpson, Wesley E. "Fast Tracking Military Waste," Civil Engineering, 59: 36-39 (April 1989).

Thibaud, Catherine, Can Erkey and Aydin Akgerman. "Investigation of the Effect of Moisture in the Sorption and Desorption of Chlorobenzene and Toluene from Soil," Environmental Science and Technology, Vol. 27 No 12: 2373-238 (1993).

Travis, Curtis C. and Jean M. Macinnis. "Vapor Extraction of Organics from Subsurface Soils: Is It Effective?" Environmental Science and Technology, Vol. 26 No 10: 1885-1887 (October 1992).

Vita

Mary Patricia (Trish) Stager was born in upstate New York in 1970. She grew up in a small town and graduated from Palmyra-Macedon High School in 1988. She attended the University of Notre Dame and graduated in 1992 with a B.S. in Civil Engineering. In 1992 she was also commissioned into the United States Air Force and first assigned to the 416th Civil Engineering Squadron at Griffiss Air Force Base, New York. There she served as a Design Civil Engineer in the Engineering flight. She also managed numerous groundwater installation and monitoring efforts in cooperation with the Environmental branch. In May 1994, Lieutenant Stager was assigned to the Air Force Institute of Technology to accomplish a Masters Degree in Engineering and Environmental Management. Following graduation, she has been appointed to a Civil/Environmental Engineering Instructor position at the United States Air Force Academy.